ULTRASTRUCTURE OF THE OPTIC NERVE MICROCIRCULATION AND LAMINA CRIBROSA IN BEAGLE DOGS WITH HEREDITARY PRIMARY OPEN ANGLE GLAUCOMA

By

DENNIS EUGENE BROOKS

A DISSERTATION PRESENTED TO THE GRADUATE SCHOOL
OF THE UNIVERSITY OF FLORIDA
IN PARTIAL FULFILLMENT OF THE REQUIREMENTS
FOR THE DEGREE OF DOCTOR OF PHILOSOPHY

UNIVERSITY OF FLORIDA

1987

ACKNOWLEDGMENTS

I would like to thank Dr. Kirk N. Gelatt for providing financial, scientific, and philosophical support for my comparative ophthalmology training. I am indebted to my electron microscopy mentor, Dr. Don Samuelson, for putting up with my impulsive work style and being patient and optimistic during the stressful periods of the experiments. Drs. Tom Kern and Dan Wolf provided me medical and surgical training. Dr. Bill Dawson encouraged me (and still does) to become a scientist and not a clinician. I am grateful to Drs. Glen Gum, Joan Dziezyc, and Patricia Smith for their friendship and unfailing support. I could not have completed the experiments without the technical support of Patricia Lewis. Becky Greene typed the dissertation in amazing fashion. Carol Haines provided much needed artistic interpretation and Kreis Weigel demonstrated his photographic prowess many times. Drs. D. J. Krahwinkel, Ron Bright and Patricia Smith pushed me to complete the work.

TABLE OF CONTENTS

	Page
ACKNOWLEDGMENTS	ii
ABSTRACT	iv
INTROOUCTION	1
Optic Nerve Damage in Glaucoma	1
POAG in the Beagle Dog	3
The Optic Nerve Lamina Cribrosa	4
Optic Nerve Capillary Ultrastructure	7
Optic Nerve Blood Supply	8
Hypotheses	9
MATERIALS ANO METHODS	11
Experiment 1: Morphologic Changes in the Lamina Cribrosa of Beagle Dogs with POAG	11
Experiment 2: Ultrastructural Changes in Laminar Optic Nerve Capillaries of Beagle Dogs with POAG	11
Experiment 3: Scanning Electron Microscopy of Corrosion Casts of the Canine Optic Nerve Microvasculature	12
RESULTS	14
Experiment 1: Morphologic Changes in the Lamina Cribrosa of Beagle Dogs with POAG	14
Experiment 2: Ultrastructural Changes in Laminar Optic Nerve Capillaries of Beagle Dogs with POAG	65
Experiment 3: Scanning Electron Microscopy of Corrosion Casts of the Canine Optic Nerve Microvasculature	106
DISCUSSION	161
SUMMARY	176
BIBLIOGRAPHY	182
BIOGRAPHICAL SKETCH	189

Abstract of Oissertation Presented to the Graduate School of the University of Florida in Partial Fulfillment of the Requirements for the Oegree of Doctor of Philosophy

ULTRASTRUCTURE OF THE OPTIC NERVE MICROCIRCULATION AND LAMINA CRIBROSA IN BEAGLE DOGS WITH HEREDITARY PRIMARY OPEN ANGLE GLAUCOMA

By

DENNIS EUGENE BROOKS

December 1987

Chairman: Dr. Kirk N. Gelatt
Cochairman: Dr. Don A. Samuelson
Major Oepartment: Veterinary Medicine

Mechanical and vascular theories have been proposed to explain the damage to optic nerve axons in human glaucoma. The optic nerve head tissues are structurally distorted posteriorly, both clinically and histologically, with prolonged elevation of intraocular pressure to result in axon compression and obstruction of axoplasmic flow. Dptic nerve vascular autoregulatory mechanisms may also be defective and result in local ischemia from circulatory abnormalities.

Optic nerve axoplasmic flow is known to be impaired at the scleral lamina cribrosa in Beagle dogs with hereditary primary open angle glaucoma and is similar to the human condition. Trypsin and detergent digests to remove all neural, vascular and glial cellular tissue revealed a well-developed scleral lamina cribrosa in the normal dog in this study. Beagle dogs with primary open angle

glaucoma demonstrated mechanical distortion of the anterior lamina cribrosa prior to the detection of ophthalmoscopic changes in the optic nerve head.

Ultrastructural examination of optic nerve capillaries in the canine lamina cribrosa revealed many spherical, membrane bound, electron-dense inclusions, that closely resembled Weibel-Palade bodies, in pericytes and endothelial cells of preglaucomatous, early, moderate, and advanced glaucomatous Beagle dogs.

Scanning electron microscopy of vascular corrosion casts of the optic nerve region in normal and glaucomatous Beagle dogs demonstrated the blood supply to the canine laminar optic nerve to be derived from short posterior ciliary arteries, cilioretinal arteries and longitudinal pial vessels. No differences between the casts in normal and glaucomatous dogs were detected.

This study revealed a significant change in the supporting architecture of the optic nerve that began early and increased in severity as the disease process progressed. An ultrastructural difference between the laminar capillary endothelial cells of normal and glaucomatous Beagles could represent a functional vascular disorder, as Weibel-Palade bodies are associated with microcirculatory abnormalities. The short posterior ciliary arteries formed a ring of striated pillars around the scleral canal. No central retinal artery was present in the dog.

INTRODUCTION

Optic Nerve Damage in Glaucoma

Primary open angle glaucoma (POAG) is a leading cause of visual impairment and blindness in humans in the U.S. POAG in man represents approximately 70% of the total of all the different types of glaucoma and is estimated to affect 2% of the population over 40 years of age.[1]

Scientific studies of glaucoma in man have been limited to clinical evaluations and histologic examination of trabeculectomy specimens or whole globes obtained from enucleation or necropsy.[2-12] Experimentally induced glaucoma models in nonhuman primates have been produced in order to study the effects of increased intraocular pressure (IOP) on the optic nerve.[8,13-16] These studies have utilized acute IOP elevations in relatively young animals and have provided interesting information in regards to tissue injury at the optic nerve, but these changes may not be entirely comparable to the human disease.[8] There is no scientific evidence to indicate that the rapid elevation in IOP causes the same mechanisms and pathologic changes at the optic nerve as the gradual pressure elevation that occurs in the natural course of the disease in man.

Controversy exists as to the pathogenesis of the damage to the optic nerve. Studies in glaucomatous human eyes,[3-5,8-11,17,18] as well as studies of experimentally induced glaucoma in nonhuman

primates,[6,15,16] cats,[19,20] and Beagles[21,22] provide evidence for the scleral lamina cribrosa as the site at which the initial pressure induced insult occurs. It is here that the axons are most concentrated and anatomically arranged to correlate with the typical, progressive visual field defects seen in humans with glaucoma.[3,9,11,23] Regional differences in the laminar pore architecture in man may explain the early selective loss of arcuate area ganglion cells and the relative preservation of foveal and nasal fibers until late in the glaucomatous disease process.[3,5,9-11] Similar regional differences in the lamina cribrosa were absent in the cat,[20] but were present in nonhuman primates.[10]

Mechanical and vascular theories have been proposed to explain the pathogenesis of the damage to optic nerve axons in glaucoma.[8,17] Elevated IOP causes inhibition of axonal flow at the lamina cribrosa in rats, dogs, cats, rabbits, nonhuman primates and humans.[11,21,22,24] The optic nerve head tissues are structurally distorted (bowed posteriorly) clinically and histologically by prolonged elevated IOP in glaucoma.[4,9,11] This mechanically induced deformation of laminar structure may cause axon compression and obstruction of axoplasmic flow in the experimental model systems and humans with glaucoma.[8,9,11,20,24] Cell death of both ganglion and glial cells is the sequelae if the IOP remains elevated. The progressive enlargement of the optic nerve cup caused by posterior displacement of the lamina cribrosa and axonal death correlates generally with the expansion of visual field defects.[8,11]

Clinical and experimental evidence suggest that insufficiency of blood flow may also play a role in glaucomatous optic nerve damage.

Anatomic distortion of the lamina cribrosa may cause compression of capillaries present within the laminar trabecular beams to result in local tissue ischemia and predispose to axonal deterioration. Deficient optic nerve vascular autoregulatory mechanisms and optic nerve vascular endothelial cell abnormalities may also lead to increased susceptibility to damage caused by elevation of IOP.[8,9,17,18,25]

Optic nerve damage in glaucoma probably reflects a disruption of the homeostatic balance between IOP and blood flow, the axoplasmic flow in the optic nerve, combinations of these and other factors, as well as the individual variation in the susceptibility of certain patients to glaucoma damage at considerably lower IOP's than others.

POAG in the Beagle Dog

Inherited POAG in the Beagle dog may possess more similarities to the human condition than any of the other currently available animal models.[2,26,27] This chronic bilateral elevation in IOP is inherited as an autosomal recessive trait. Beagles with early POAG (6-12 months of age) demonstrate IOP of 30-35 mmHg, an open iridocorneal angle, reduced tonographic (C) values (C value = 0.12 microliters/mmHg/min; normal values = 0.24 microliters/mmHg/min) and a normal optic nerve head. With moderate untreated glaucoma (13-30 months of age), the iridocorneal angles are slightly narrowed, although still open gonioscopically. The IOP is 50 mmHg or greater with the facility of aqueous outflow further reduced. Variable amounts of optic disc cupping are present, and focal disinsertion of the lens zonules is noted. Some affected Beagles demonstrate loss of

the lateral optic disc rim while others have central to paracentral cupping of the optic disc. Beagles with advanced untreated glaucoma (greater than 31 months of age) exhibit narrow to closed iridocorneal angles, further decreased facility of outflow, elevated IOP (75 mmHg) and anterior or posterior lens luxation with cataract formation.[26] Corneal edema, episcleral congestion, buphthalmos, and retinal degeneration occur as the disease progresses. Peripapillary retinal blood vessels gradually disappear, and the optic discs become round, depressed and not infrequently pigmented in the eyes of affected Beagles at the advanced stage of disease. Early optic nerve cupping can be demonstrated with serial photographs and progresses to optic nerve atrophy at approximately 48 to 72 months of age.[1,2,26] Axoplasmic flow has been documented by autoradiography to be impaired at the scleral lamina cribrosa in Beagles with POAG.[21,22] This correlates to the ultrastructural changes seen in humans and experimental animal models.[8,9] Damage to axons and glial cells of the glaucomatous Beagle was substantial and progressive.[22]

The Optic Nerve Lamina Cribrosa

The anterior or choroidal lamina cribrosa is composed of the axons of the retinal nerve fiber layer which are arranged into bundles of nerve fibers as they approach the optic nerve head and are surrounded by tube-like glial channels formed by astrocytes. This loose glial connective tissue contains capillaries and forms trabeculae between the nerve fiber bundles in order to provide support for the nerve fibers as they make a 90° bend into the scleral canal from the retinal nerve fiber layer to form the optic nerve.[6,23]

The posterior scleral part of the lamina cribrosa is derived from the meridional extensions of the sclera.[6] Numerous oval or round perforations are present in the concentric sheets of connective tissue that bridge the scleral canal. These perforations are aligned between successive laminar sheets to form passages for the nerve fiber bundles. Astroglia extend around the rim of each opening to form a continuous glial membrane around each nerve fiber bundle, thus separating the nerve fiber bundles from the adjacent connective tissues. Each connective tissue trabeculae has a capillary in its center. Optic nerve head capillaries are nonfenestrated with tight junctions between adjacent endothelial cells.[6,23]

In nonhuman primates, centripetal branches from the short posterior ciliary arteries (SPCA) supply the lamina cribrosa. A dense, widely anastomotic capillary plexus is present within the connective tissue septa.[28] All the capillaries in the optic nerve head are interconnected, being continuous posteriorly with those of the retrolaminar region and anteriorly with the adjoining retina.[28]

A tissue digestion technique was utilized in glaucomatous human globe specimens to examine the lamina cribrosa.[4,9] Detergent and trypsin digested optic nerve tissues were examined by transmission and scanning electron microscopy. Transmission electron microscopy revealed the presence of connective tissue with a near total absence of cells. Astrocyte and capillary basement membranes were intact. Scanning electron microscopy demonstrated large pores in the superior and inferior portions of the scleral lamina cribrosa, with thinner connective tissue support for the passage of the optic nerve fiber bundles than in the nasal and temporal parts of the lamina cribrosa.

These regional differences in the anatomy of the lamina cribrosa may explain the relative vulnerability of the arcuate area ganglion cell axons to glaucoma damage as they pass through the superior and inferior laminar zones.[4] Misalignment of these pores may, in turn, cause obstruction of axoplasmic flow.[4,8]

Examination of trypsin digested human eyes revealed that mechanical compression of the lamina cribrosa occurred prior to the detection of visual field defects. Increased IOP caused the lamina cribrosa to arch posteriorly and resulted in the misalignment of the pores within the layers of the lamina through which the axon bundles pass. The anatomic disruptions of the lamina cribrosa occurred very early in the disease process and were considered a primary pathogenic event.[5]

The cat, monkey and squirrel have a well-developed lamina cribrosa with collagen fibers. The lamina of the mouse and rabbit is poorly developed with no collagen connective tissue present at the site of the lamina.[29] The lamina cribrosa of the rat consists of one perforated sheet crossing the scleral canal.[24]

In the feline lamina cribrosa, the nerve fiber bundles are larger and the trabecular tissue finer in the temporal region than the nasal region;[19] this was not correlated with damage to the temporal optic nerve in the experimental hypertensive axonal transport interruption.[20] Autoradiography revealed that the lamina cribrosa was the site of optic nerve axonal transport blockade in the experimentally hypertensive feline globe.[20]

Optic Nerve Capillary Ultrastructure

Autoradiographic and ultrastructural studies of the optic nerve of glaucomatous Beagles and nonhuman primates have revealed swollen axons with accumulation of cellular organelles at the scleral lamina cribrosa, axonal demyelination, and glial cellular changes.[8,9,11,21,22] Axonal and glial cell abnormalities may be associated with the mechanically induced axoplasmic transport blockage or local tissue ischemia. It has been recently proposed that the endothelial cells of the optic nerve microvasculature may be inherently functionally abnormal in human patients with glaucoma.[25] Defective control of vascular perfusion resistance or other abnormalities in the microvasculature could result in increased local vascular insufficiency and abnormal permeability in response to glaucoma-associated mechanical changes in the lamina cribrosa and optic nerve.

Detection of endothelial cell, pericyte, basement membrane, and cytoplasmic abnormalities in Beagles with early glaucoma would suggest that not all the axonal and glial cellular changes noted in the Beagle are the result of simple mechanical distortion of the lamina cribrosa. Inherently abnormal vascular endothelial cells in the optic nerve may influence arteriolar smooth muscle cell function in an inappropriate manner such that blood flow is insufficient to the axons and glial cells during sustained elevations of IOP. Any ultrastructural morphologic changes noted between normal and affected dogs with chronically elevated IOP would indicate that the microvascular changes have, in part, a structural basis, rather than being a purely functional disorder. Precise functional studies are difficult to

perform on the circulation of such a small area, so I have chosen to examine the ultrastructural morphology of the optic nerve laminar capillaries. The presence of increased numbers of tubular bodies, decreased mitochondrial content, and multilaminated, thickened basement membrane (BM) in capillary endothelial cells has been used to indicate abnormal microvascular function and has been associated with several pathologic conditions.[30-32] Predicting the degree of dysfunction from abnormal ultrastructural appearance is speculative but is a reasonable approach. Although abnormal appearance may suggest that a tissue disorder exists, any vascular changes seen could be secondary to local tissue pathology or vice versa.

Optic Nerve Blood Supply

The microvasculature of the anterior optic nerve head of primates is rich and highly anastomotic.[33] The blood vessels of the human and nonhuman primate optic disc are anatomically and ultrastructurally similar to the retina-optic nerve microvasculature system, but not the adjacent choroidal vessels.[28] The prelaminar optic nerve in man and nonhuman primates derives its blood supply from centripetal branches of short posterior ciliary arteries. Optic disc capillaries are continuous with retinal capillaries, but do not communicate with the choroidal capillary bed, the choriocapillaris.[28,34] The human and nonhuman primate lamina cribrosa receives longitudinal pial arterioles from the retrolaminar optic nerve and transverse arterioles from the scleral posterior ciliary arteries.[28,34]

The optic nerve microcirculation of the sheep,[35] rat[36] and cat[37,38] has also been studied. The arterial supply to the

prelaminar optic nerve and lamina cribrosa of the dog is more anecdotal than precisely defined.[39,40]

The blood supply of the anterior optic nerve has been studied by plastic and rubber injection techniques,[34-38,41] microradiographic dyes[42] and systematic histologic methods.[33,43] Scanning electron microscopy of corrosion casts provides precise three-dimensional replicas of vascular spatial relationships which can be viewed at high magnification, resolution and depth of field in order to accurately describe microvascular systems.[34,36,38,44-53]

Hypotheses

The trypsin and detergent digest techniques enzymatically remove all neural and glial cellular elements of the optic nerve, leaving only connective tissue.[4,5] The first experiment will examine the optic nerve of normal and glaucomatous Beagle dogs to determine if structural alterations of the lamina cribrosa occur early in the disease and become worse as the glaucoma progresses. Structural misalignment of the scleral lamina cribrosa could contribute to blockage of optic nerve axoplasmic flow.

The second experiment will determine if the laminar optic nerve capillary endothelial cells are ultrastructurally abnormal, compared to age-matched normal dogs and acutely ocular hypertensive experimental dogs, prior to and during the chronic elevations in intraocular pressure seen in Beagles with POAG. Deficits in vascular endothelial cell function could therefore be present in the early phase of the glaucomatous disease process if such abnormal morphology is present. Elucidation of the time course of microvascular

ultrastructural abnormalities will provide more precise evidence for any causal relationship between the elevated intraocular pressure and the damage to optic nerve axons and glial cells. Interpretation of cellular ultrastructural abnormalities of the optic nerve capillaries will be aided by other studies.[33, 54-62] The optic nerve capillaries are continuous when in contact with axons and fenestrated when in contact with the interstitial connective tissue.[60]

Morphological study is a basic prerequisite for understanding the normal functioning of an organ or structure. The third experiment is to document the vascular channels supplying the anterior optic nerve region in the normal Beagle dog. Beagles with hereditary primary open angle glaucoma will also be studied using scanning electron microscopic examination of corrosion casts in order to detect any alterations in the three dimensional angioarchitecture of the glaucoma damaged optic nerve.

MATERIALS AND METHODS

Experiment 1: Morphologic Changes in the Lamina Cribrosa of Beagle Dogs with POAG

Five normal, one acute ocular hypertensive, and eight glaucomatous Beagles (one preglaucoma, one early, four moderate, two advanced) were evaluated by ophthalmoscopy, biomicroscopy, tonometry, fundus photography, and fluorescein angiography prior to morphologic studies.

Glutaraldehyde (2.0%, 0.1 M cacodylate buffer, pH 7.2) perfusion fixed optic nerve hemisections were digested at 37° C in 3% trypsin in 0.15 M hydroxymethyl aminomethane (tris) buffer (pH 7.8) for approximately 12 hours. The tissue was then rinsed in buffer, immersed in 20% acetylcysteine, subjected to ultrasound for 15 minutes and rinsed again in buffer. The tissue was then dehydrated in a graded series of ethanol and critical point dried with liquid CO_2. The tissue pieces were then mounted on aluminum stubs, vacuum coated at 10^{-4} torr, with 200 Angstrom thickness of gold-palladium, and examined with the JEOL SEM 35C.

Experiment 2: Ultrastructural Changes in Laminar Optic Nerve Capillaries of Beagle Dogs with POAG

Four normal, two acute ocular hypertensive dogs, and eight glaucomatous Beagles (one preglaucoma, one early, four moderate, two advanced) were evaluated by ophthalmoscopy, biomicroscopy, tonometry,

fundus photography and fluorescein angiography prior to anatomic studies. All globes were arterially perfused with glutaraldehyde immediately post-enucleation. Glutaraldehyde perfusion fixed optic nerve hemisections were osmicated, dehydrated in a graded ethanol series and embedded in epon-araldite. One micron sections were prepared and stained with Toluidine blue in order to localize the laminar region. Randomly sampled longitudinal and transverse ultrathin (600A) sections of each optic nerve hemisection were mounted on grids, post-stained, and the capillaries of age-matched normal, acute ocular hypertensive, and affected Beagles examined by transmission electron microscopy (TEM).

Experiment 3: Scanning Electron Microscopy of Corrosion Casts of the Canine Optic Nerve Microcirculation

Four normal and two affected Beagles with POAG (one moderate, one advanced) were evaluated by ophthalmoscopy, biomicroscopy, tonometry, fundus photography, and fluorescein angiography prior to the morphologic studies.

The common carotid arteries and jugular veins were cannulated following general anesthetic (halothane and oxygen) induction. Saline (0.9% N) solution was perfused through the carotid arteries, to remove the blood and prevent vasospasm, until clear effluent exited the jugular veins. Batson's compound (methylmethacrylate corrosive compound #17) was mixed with Sevriton acrylic filling material in order to produce a suitable low viscosity cast medium for fine vessels. Sixty milliliters of this mixture was rapidly injected by syringe using hand pressure until the compound egressed from the

jugular veins. The head was placed in an ice bath and allowed to "set" for two hours. The globe and nerve were then excised and allowed to "set" for another 8-12 hours. The globe specimens were then macerated in 40% KOH at 60° C for 48 hours. The KOH was changed twice a day and the resulting castings air dried in a dessicator. The posterior segment was then coated with gold palladium in a Hummer I sputtering apparatus and examined with the JEOL SEM 35C.

RESULTS

Experiment 1: Morphologic Changes in the Lamina Cribrosa of Beagle Dogs with POAG

Normal Dogs

The scleral lamina cribrosa was well developed in the normal adult dog (Fig. 1-9a). It was composed of 10-15 sheets of collagenous connective tissue that bridged the scleral canal. Many pores were noted in each sheet, varying in size from 12 to 50 microns. Spaces between the lamellae in normal dogs were about 25 microns. Remnants of axon bundles make a 90° turn from the retinal nerve fiber layer to form the optic nerve.

The glial framework of the nerve fiber layer occupied the entire anterior optic nerve head and accounted for the large volume of the optic nerve head. Undigested vascular basement membrane was on the anterior surface of the optic nerve head. The choroidal capillary basement membranes formed a mosaic appearance on the anterior surface of the specimens. The axonal tracts of the optic nerve head caused it to protrude above the anterior retinal surface.

The scleral lamina cribrosa possessed many perforations and the congruent perforations of successive lamellae were aligned to form passages for the nerve fiber bundles. Some nerve fiber bundle remnants were seen to linearly traverse the many layers of the lamina cribrosa. Some of the nerve fiber bundles branched within the lamina

cribrosa to send part of their fibers through different laminar fenestrations. The wide spacing of the normal laminae was quite evident. No differences in pore size could be detected between the nasal/temporal or dorsal/ventral quadrants.

Glaucoma Dogs - Experimental Hypertensive and Hereditary POAG

Ultrastructural morphologic changes occurred in the prelaminar, laminar and retrolaminar regions. No changes were noted in a preglaucomatous (3 month old) Beagle (Fig. 9b). Slight distortion of the lamina cribrosa was noted in a Beagle with early glaucoma, prior to overt ophthalmoscopic changes in the optic nerve head (Fig. 10).

Beagles with the moderate stage of glaucoma (Fig. 11-16) had some posterior displacement of the lamina cribrosa and slight compression of the laminae with an interlaminar space of about 10 microns. Although pore misalignment was present, axons in the center of the nerve of one animal did not appear to be compromised. Tissue from an acutely hypertensive dog (75 mmHg) (Fig. 17, 18) revealed changes similar to the moderately affected Beagles.

Beagle dogs with advanced stages of glaucoma demonstrated severe alterations of the laminar architecture (Fig. 19-24). The anterior surface of the optic nerve hemisection was bare with no recognizable surface structures. Extreme posterior displacement of the lamina was manifested by optic nerve cupping ophthalmoscopically, and electron microscopic evidence of near total obliteration of laminar pore space, compression of the laminae, and distortion of congruent pores. The position of the vascular basement membrane remnants demonstrated an extreme amount of cupping. Little space was available for the

passage of neural tissue. Interestingly, the optic nerve of one Beagle that was classified clinically as advanced, resembled those of a moderately affected dog. No regional differences in the lamina to explain increased susceptibility to the elevated IOP were detected.

FIGURE 1. SCANNING ELECTRON MICROSCOPY OF NORMAL TRYPSIN DIGESTS. a. Hemisection of optic nerve revealed undigested vascular basement membrane on the anterior optic nerve surface, the fine meshwork of the retinal lamina cribrosa, wider spacing of the choroidal lamina cribrosa, and the skeletal framework of the axon bundles. (53 X.) b. Close-up of Fig. 1a of the central choroidal optic nerve is seen. Note the wide-spacing of the laminae and the collagen support tissue of the axon bundles. (250 X.)

1a

b

FIGURE 2. SCANNING ELECTRON MICROSCOPY OF NORMAL TRYPSIN DIGESTS. a. Axon bundles move through the trabeculae of the lamina cribrosa. (250 X.) b. Note the longitudinal axon bundles (a) and transverse trabecular collagen laminae (b) in this micrograph. (2500 X.)

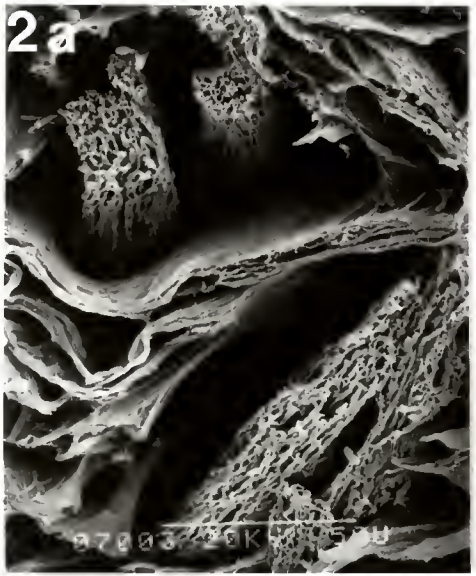
2a

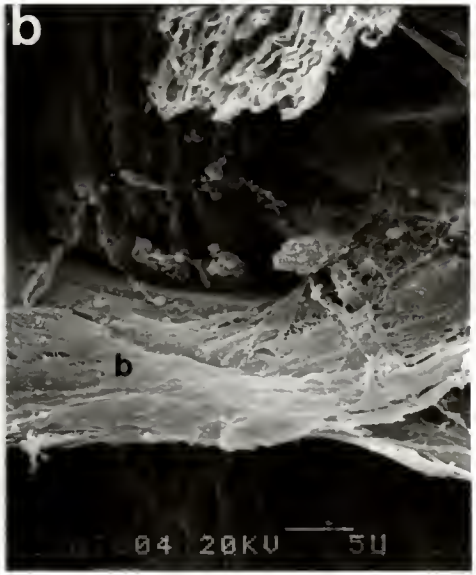
b
b
04 20KV 5U

FIGURE 3. SCANNING ELECTRON MICROSCOPY OF NORMAL TRYPSIN DIGESTS. a. Cross section from the central region of the optic nerve shows several axon bundles passing through the lamina. Wide spaces are pronounced. (250 X.) b. Tissue depicted on this micrograph is more posterior in the lamina and shows more abundant collagen in the axon bundles (a). Spaces between axons and the lamina are still prominent. (250 X.)

b
a
a
a
a
5 μm

3a

FIGURE 4. SCANNING ELECTRON MICROSCOPY OF NORMAL TRYPSIN DIGESTS. The collagen framework of the axons and lamina is illustrated. (750 X.) b. Vascular basement membrane remnants (arrows) are prominent on the anterior surface of the optic nerve head. (90 X.)

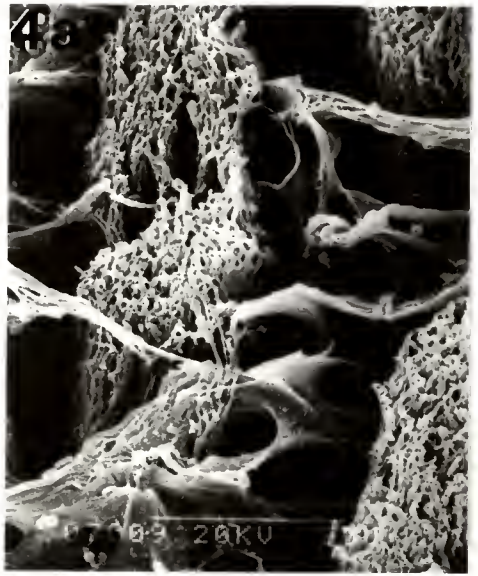
4a
20KV

b
07010 20KV 500U

FIGURE 5. SCANNING ELECTRON MICROSCOPY OF NORMAL TRYPSIN DIGESTS. a. Central anterior optic nerve has axon bundle remnants in the pores of the laminar beams. (400 X.) b. Optic nerve hemisection showing wide-spacing of lamina cribrosa. (100 X.)

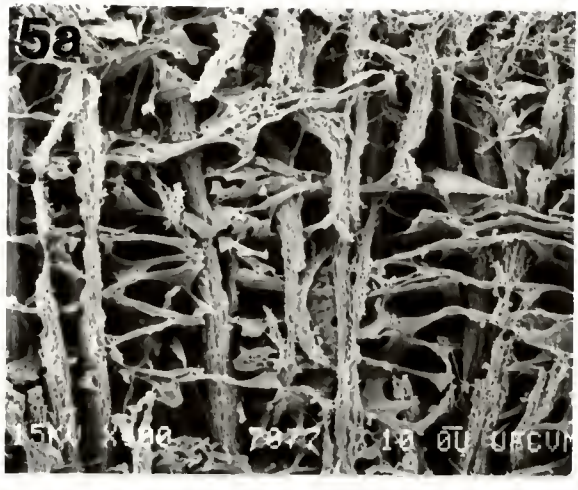
5a

б

FIGURE 6. SCANNING ELECTRON MICROSCOPY OF NORMAL TRYPSIN DIGESTS. Close-up view of the lamina cribrosa reveals many open spaces near axon bundles. Spaces narrow near the edge of the scleral canal (arrows). (360 X.) b. Several axon bundle remnants are noted passing through the laminar region. (320 X.)

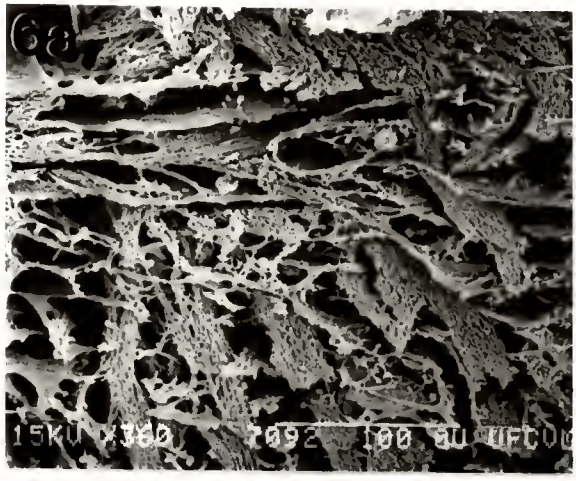
68
15KU X360 7092 100 SU UFCU

15KU X320 7073 100 SU UFCU

FIGURE 7. SCANNING ELECTRON MICROSCOPY OF NORMAL TRYPSIN DIGESTS. a. Remnants of axon bundles can be seen passing through widely spaced pores of the lamina cribrosa. (480 X.) b. Choroidal capillary basement membranes form a mosaic appearance on the anterior surface of the specimen. (260 X.)

7a

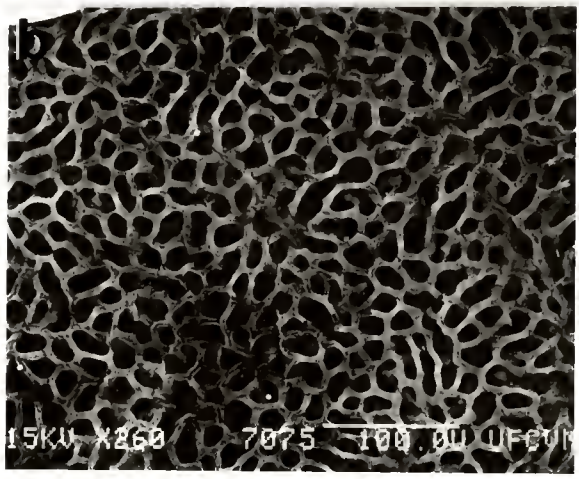
b
15KV X260 7075 100.00 UFCU

FIGURE 8. SCANNING ELECTRON MICROSCOPY OF NORMAL TRYPSIN DIGESTS. a. Wide spaces of normal lamina cribrosa are seen. (50 X.) b. Anterior optic nerve head appears fibrous due to remnants of axons and vascular basement membrane (arrow). (50 X.)

8a
07015 25KV 500U

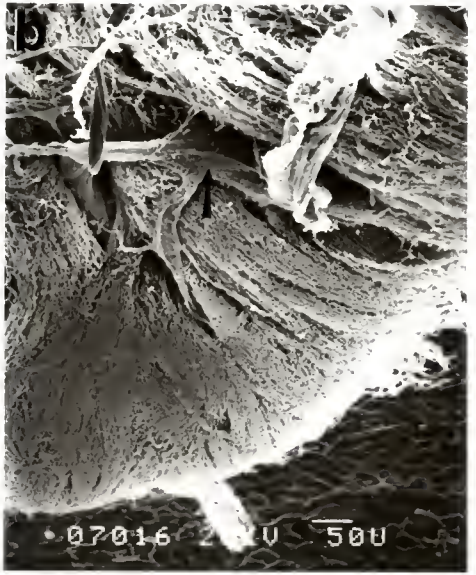
b
07016 500U

FIGURE 9. SCANNING ELECTRON MICROSCOPY OF NORMAL AND PREGLAUCOMATOUS TRYPSIN DIGESTS. a. The supporting collagen structure of the lamina cribrosa is arranged parallel to each adjoining layer (Old normal, 200 X.) b. The lateral edge of the lamina cribrosa contains wide spaces, but the tissue of younger dogs did not digest well. (preglaucoma, 220 X.)

9a
15KV X23 7068 100.0U UFCVM

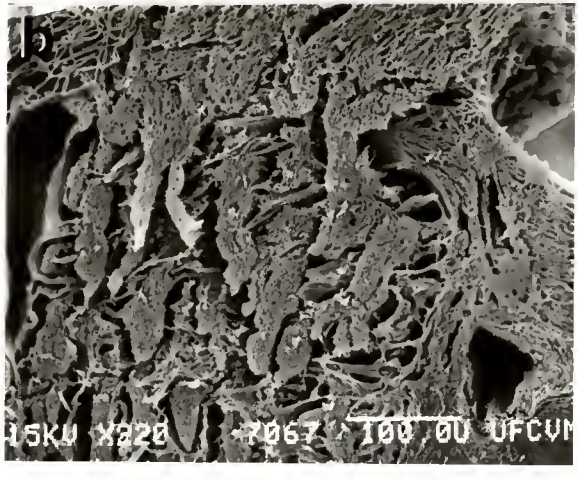
15KV X320 7067 100.0U UFCVM

FIGURE 10. SCANNING ELECTRON MICROSCOPY OF EARLY GLAUCOMA DETERGENT DIGEST. The detergent digest technique failed to remove as much tissue as the trypsin digest method. Some neural tissue on the anterior surface is digested to reveal vascular basement membranes. (120 X.)

10
27003 20KV 50U

FIGURE 11. SCANNING ELECTRON MICROSCOPY OF MODERATE GLAUCOMA TRYPSIN DIGESTS. a. Some compression and posterior displacement of the lamina cribrosa is evident (arrow). (200 X.) b. Alteration of the laminar architecture is present (arrow). (160 X.)

11a

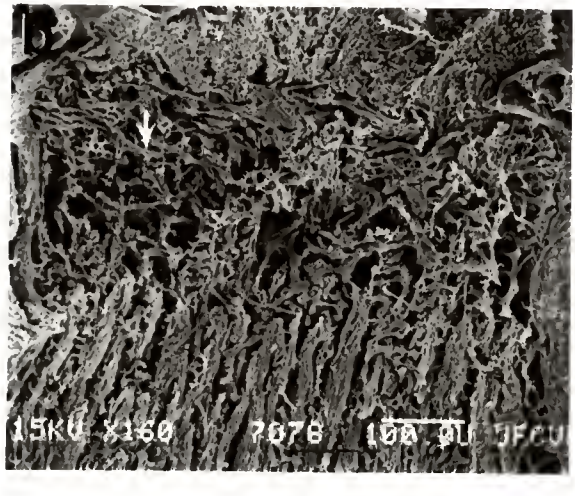
15KV X160 7078 100 UU

FIGURE 12. SCANNING ELECTRON MICROSCOPY OF MODERATE GLAUCOMA TRYPSIN DIGESTS. a. This view of the anterior laminar area reveals marked alteration of laminar geometry. (320 X.) b. Some pore misalignment is evident although an axon bundle can be seen in the center that does not appear to be affected (arrow). (660 X.)

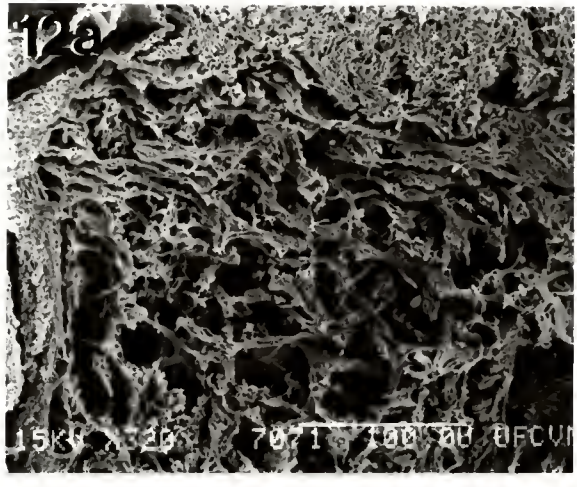
12a

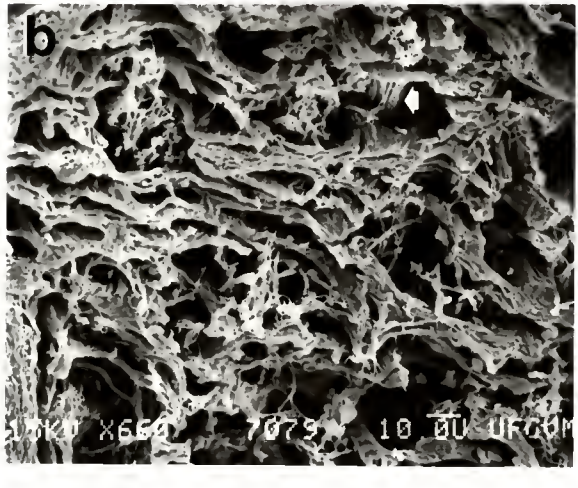
b

FIGURE 13. SCANNING ELECTRON MICROSCOPY OF MODERATE GLAUCOMA TRYPSIN DIGESTS. a. Several axon bundles are passing through pores of the lamina cribrosa. Anterior laminar compression is noted. (66 X.) b. Axon bundles can be seen passing through several laminar areas. A vascular basement membrane remnant is present (arrow) (200 X.)

13a
20KV X66 7022 100.0U UFCVM

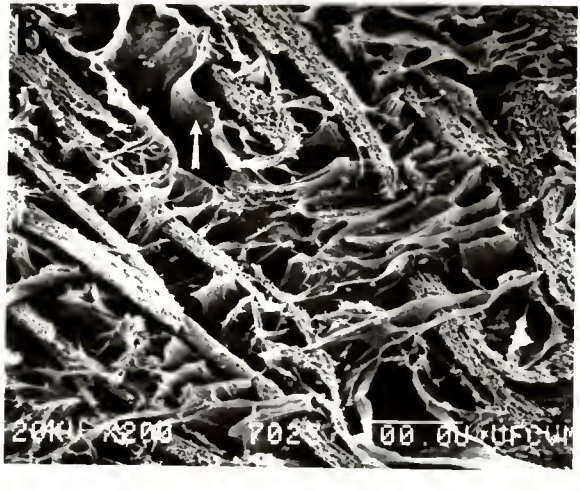
b

FIGURE 14 SCANNING ELECTRON MICROSCOPY OF MODERATE GLAUCOMA TRYPSIN DIGESTS. a. Optic nerve head is viewed from the anterior surface. It protrudes above the retinal surface. Note pattern of choroidal capillary basement membrane (star). (78 X.). Lateral view of optic nerve hemisection shows laminar compression and disorganization (arrow). (200 X.)

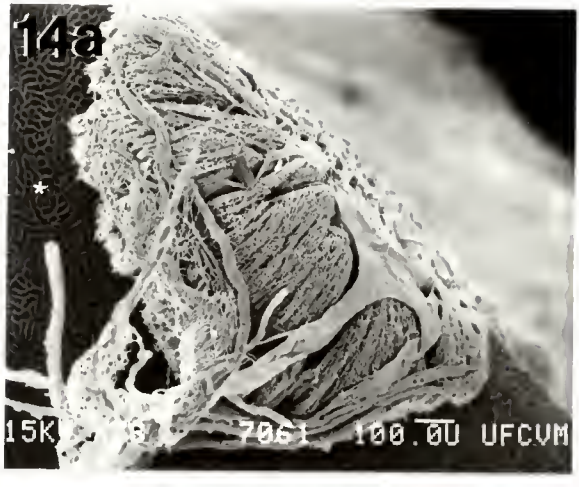
14a
15K
7061
100.0U UFCVM

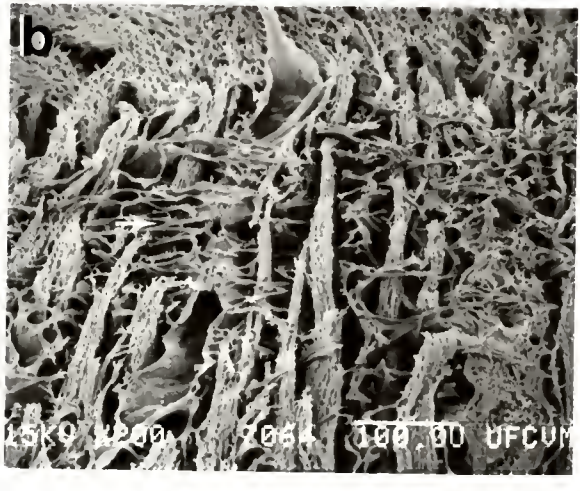
b
15KO
7064
100.0U UFCVM

FIGURE 15. SCANNING ELECTRON MICROSCOPY OF MODERATE GLAUCOMA TRYPSIN DIGESTS. a. Axon passing through a compressed laminar pore. (660 X.) b. Laminar compression and pore distortion is evident. (175 X.)

15a
7065

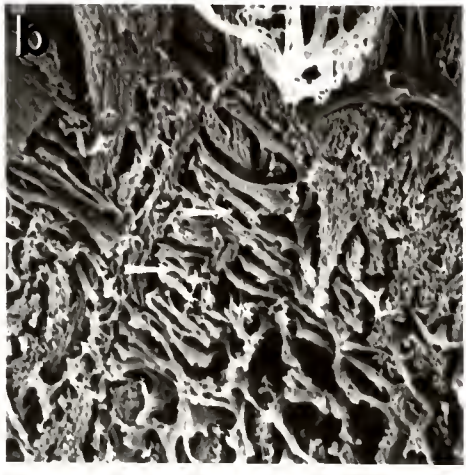
b

FIGURE 16. SCANNING ELECTRON MICROSCOPY OF MODERATE GLAUCOMA TRYPSIN DIGEST. Posterior movement and distortion of laminar beams is present. (500 X.)

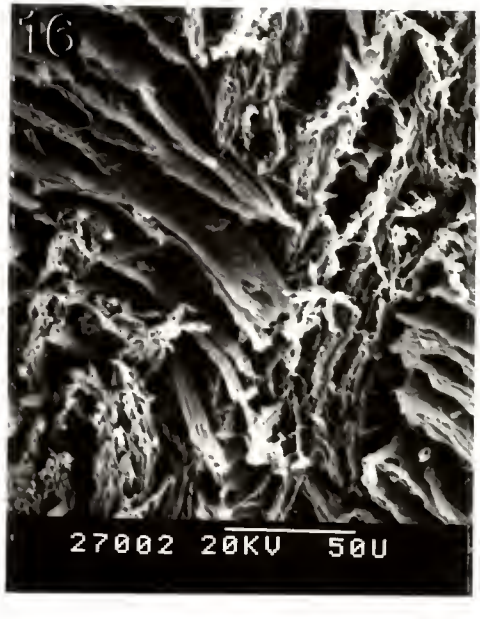
16
27002 20KV 50U

FIGURE 17. SCANNING ELECTRON MICROSCOPY OF EXPERIMENTAL HYPERTENSIVE TRYPSIN DIGESTS. a. An optic nerve axon passes through several pores. Some posterior displacement of the edge of the lamina is noted. (300 X.) b. The anterior edge of the lamina is compressed (arrows). (150 X.)

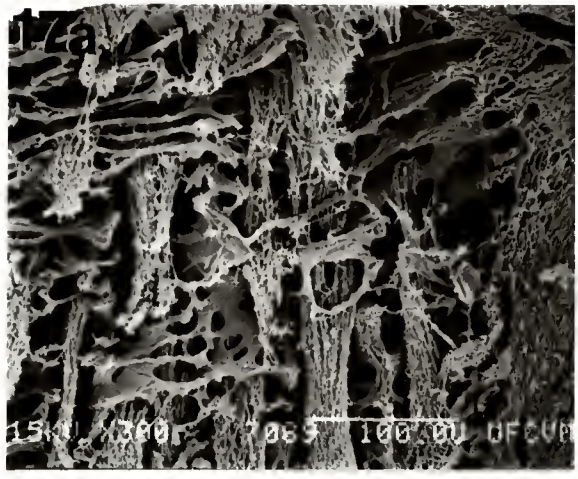
100.0U UFCVM

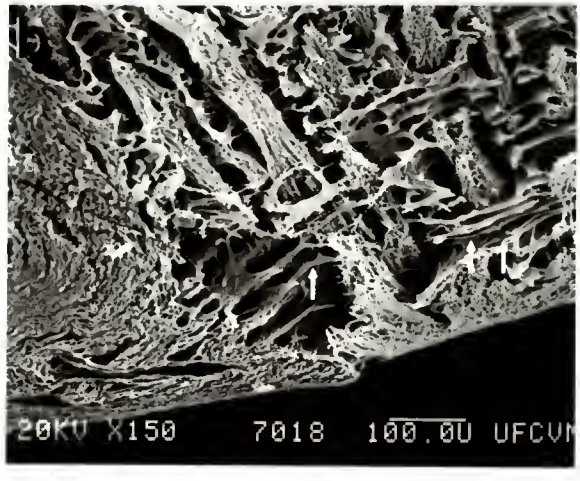
20KV X150 7018 100.0U UFCVM

FIGURE 18. SCANNING ELECTRON MICROSCOPY OF EXPERIMENTAL HYPERTENSIVE TRYPSIN DIGESTS. a. Many optic nerve axon bundles are present in the retrolaminar area. (200 X.) b. The overall view of an optic nerve hemisection is shown (78 X.)

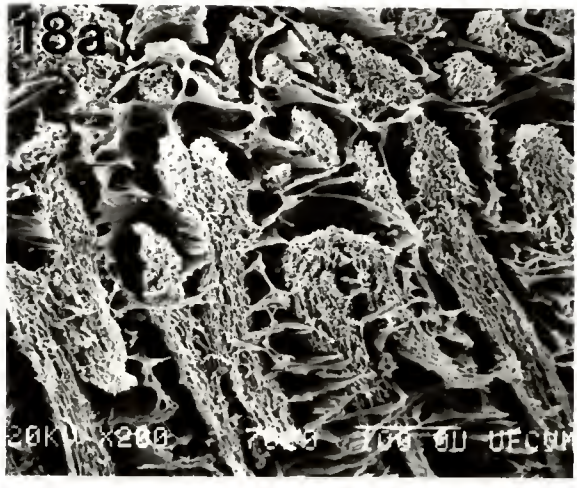
18a

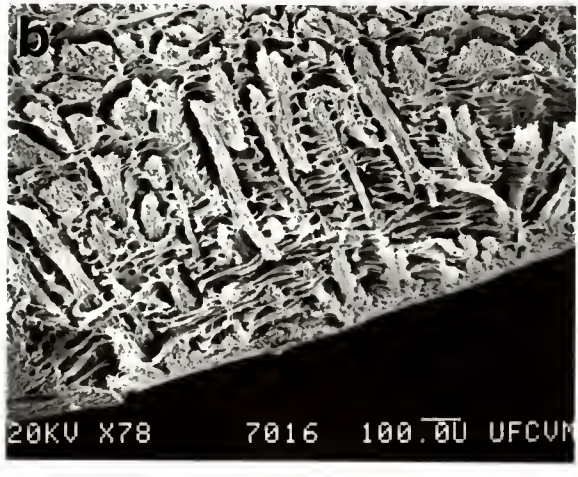
b
20KV X78 7016 100.0U UFCVM

FIGURE 19. SCANNING ELECTRON MICROSCOPY OF ADVANCED GLAUCOMA TRYPSIN DIGESTS. a. Marked laminar compression and optic nerve cupping are present (arrow marks anterior edge). (86 X.) b. More magnified view of Fig. 19a showing laminar compression and pore distortion. Note the vascular basement membranes on the optic nerve surface. (200 X.)

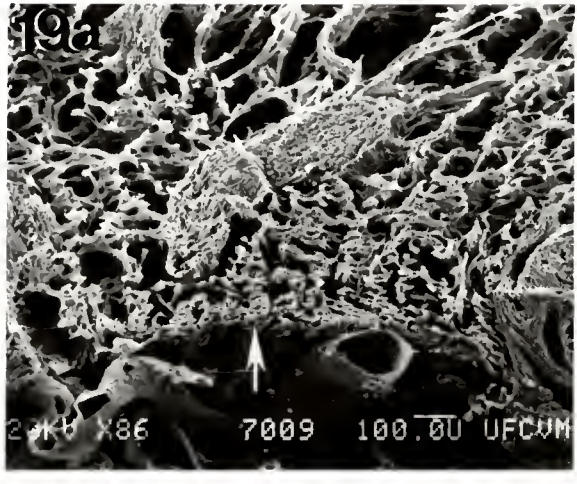
19a
20KV X86 7009 100.0U UFCUM

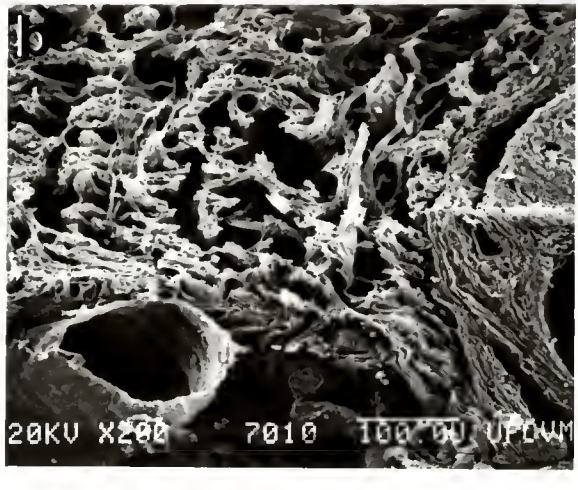
b
20KV X200 7010 100.0U UFCUM

FIGURE 20. SCANNING ELECTRON MICROSCOPY OF ADVANCED GLAUCOMA TRYPSIN DIGESTS. a. Many vascular remnants are noted on the anterior surface of the optic nerve head. A short posterior ciliary artery is present (star). (200 X.) b. Retrolaminar distortion appears to be minimal. (150 X.)

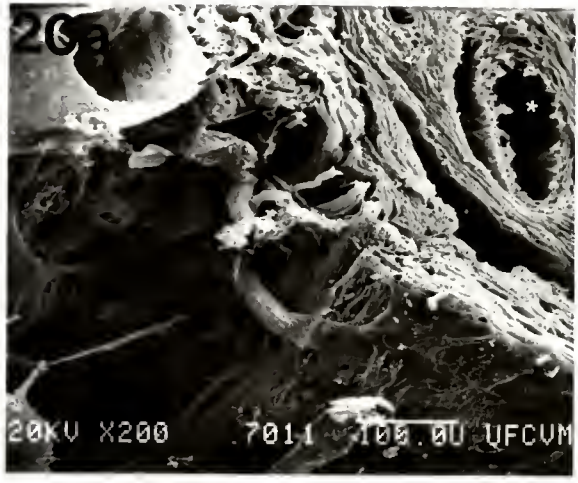
20KV X200 7011 100.0U UFCVM

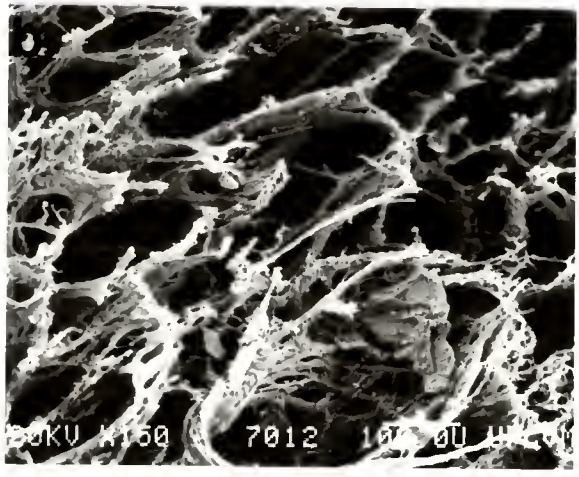
7012

FIGURE 21. SCANNING ELECTRON MICROSCOPY OF ADVANCED GLAUCOMA TRYPSIN DIGESTS. a. This optic nerve hemisection reveals severe posterior displacement of the anterior optic nerve head. (60 X.) b. Marked laminar distortion with obliteration of pores is apparent. (110 X.)

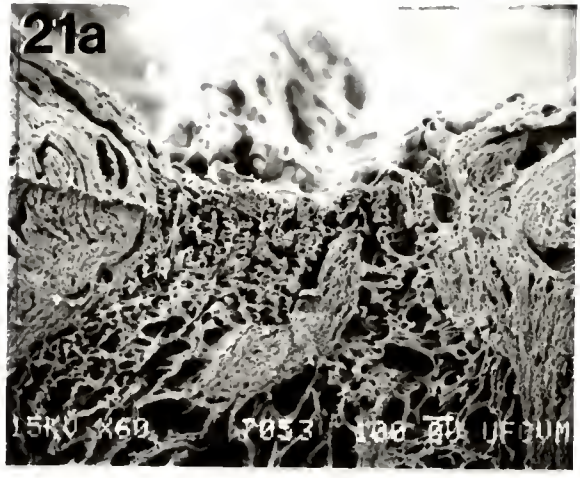
21a
15KV X60 7053 100 UFCUM

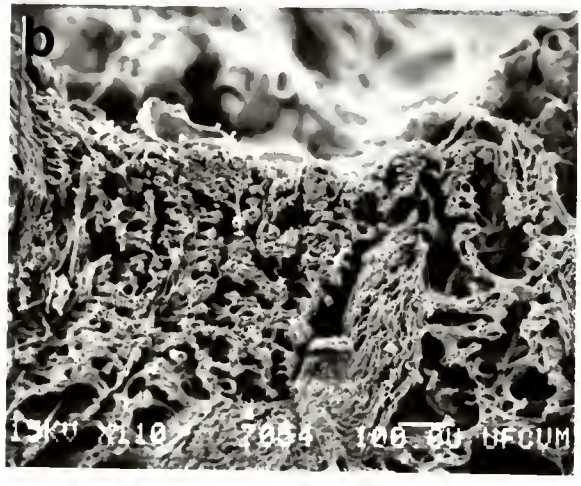
b
UFCUM

FIGURE 22. SCANNING ELECTRON MICROSCOPY OF ADVANCED GLAUCOMA TRYPSIN DIGESTS. a. The anterior laminar area is severely altered structurally. (200 X.) b. Laminar beams are pressed closely together in the anterior (arrows) lamina cribrosa. (480 X.)

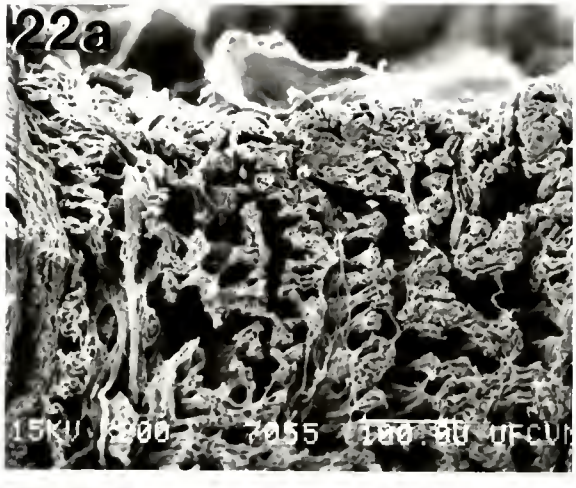
22a
15KV X300 7055 100.00 UFCUM

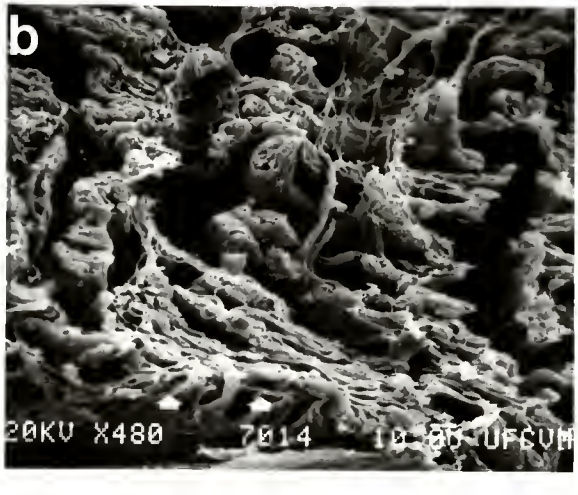
b
20KV X480 7014 10.00 UFCUM

FIGURE 23. SCANNING ELECTRON MICROSCOPY OF AOVANCED GLAUCOMA TRYPSIN OIGESTS. a. The anterior face of this optic nerve hemisection is seen. The vascular basement membrane remnants demonstrate the large amount of cupping present. (78 X.) b. Closeup of anterior surface of the lamina cribrosa. No recognizable normal architecture is present. The surface of the lamina cribrosa is bare. There is little space for passage of axon bundles. (400 X.)

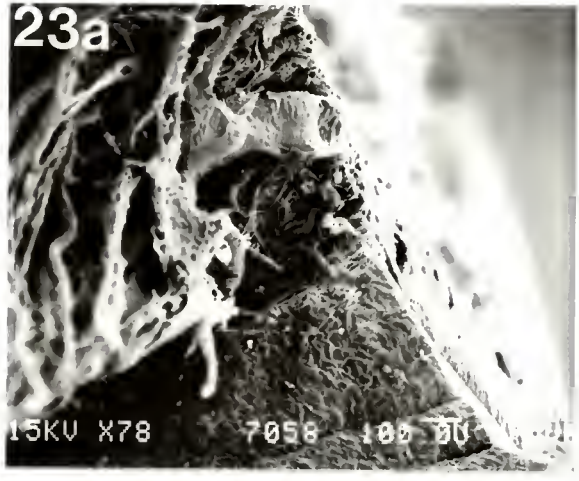
23a
15KV X78
7058

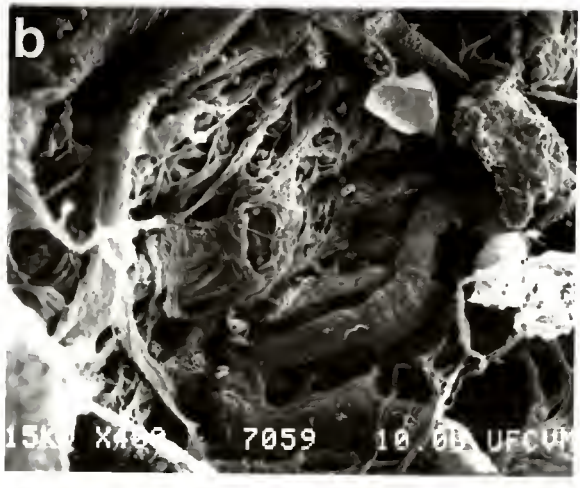
b
7059

FIGURE 24. SCANNING ELECTRON MICROSCOPY OF ADVANCED GLAUCOMA TRYPSIN DIGEST. The entire digested lamina is shown. Severe cupping is present. Note compression of anterior layers (arrows). (72 X.)

24

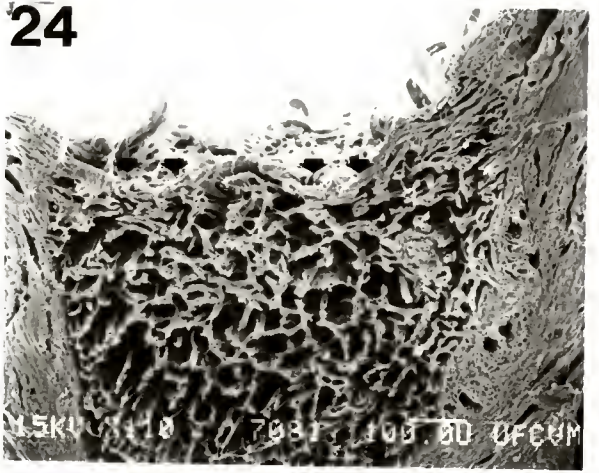

Experiment 2: Ultrastructural Changes in Laminar Optic Nerve Capillaries of Beagle Dogs with POAG

Preglaucoma

One 3-month-old affected Beagle was examined. Many spherical, membrane bound, electron-dense inclusions were seen in the endothelial cell cytoplasm of trabecular beam capillaries (Fig. 1a, 1b). The inclusions were 0.5-1.0 microns in diameter. Pericyte and endothelial cell nuclei appeared normal. A circular translucent round structure was seen in some of the electron-dense inclusions(Fig. 1c, 1d). Collagen fibers clearly surrounded each capillary examined.

Early Glaucoma

One affected Beagle in this category was available for study. Few electron-dense membrane bound inclusions were noted in the endothelial cell and pericyte (Fig. 2a, 2b) cytoplasm. Large vacuolated regions were extensive and present in the endothelial cell cytoplasm (Fig. 2c, 2d, 3a). The endothelium appeared swollen and edematous with disrupted cell membranes (Fig. 2a). Free ribrosomes appeared decreased in quantity (Fig. 3b). The lumen of some capillaries contained red blood cells.

Moderate Glaucoma

Four affected Beagles at this stage of glaucoma were examined. The endothelial cytoplasm was filled with spherical and tubular membrane bound (0.6-3.2 microns) electron-dense inclusions (Fig. 4, 5, 6a). Vacuolization was present in some endothelial cells (Fig. 6b). Internal structuralization manifested by round translucent

areas in the electron-dense inclusions was present (Fig. 6c). Pericytes also contained electron-dense inclusions and degenerating organelles, that were possibly mitochondria (Fig. 5c, 6d, 7a). The collagen framework of the laminae were abnormal (breaking up) in some sections (Fig. 7b). Lipid deposits were noted in some endothelial cells (Fig. 4b, 5d). Blunting of the microvillous projections into the capillary lumen occurred (Fig. 7c). Endothelial basement membrane thickness was 0.4 microns.

Advanced Glaucoma

Two affected Beagles were examined. Capillaries contained a few (Fig. 8a, 8b) to many (Fig. 8c-9) membrane bound electron-dense inclusions in the endothelial cell cytoplasm. The inclusions were 0.2-2.7 microns in size. Circular transparent regions were present in some membrane bound inclusions (Fig. 10a). The capillary lumens were collapsed in several of the sections of one perfused specimen (Fig. 10b-d). Cystic mitochondria were in axons with degenerating myelin sheaths (Fig. 10d-11b). Other vacuolizations were noted (Fig. 11c).

Many pinocytotic vesicles opened into the capillary lumen (Fig. 11d). Large (1.2 micron) endothelial vacuoles may represent degenerating mitochrondria as cristae appeared in some cells (Fig 10a). Fewer free ribosomes and rough endoplasmic reticulum (ER) were observed (Fig. 10c, 12a). Autophagosomes were present (Fig. 13c) in the cytoplasm of some endothelial cells.

Microvilli with microfilaments were severely reduced in number, but many pinocytotic vesicles were present (Fig. 12b, 12c, 9b).

Interendothelial cell processes were swollen and blunted in some specimens (Fig. 12c). Platelets and red blood cells were present in some lumens (Fig. 8a, 12c).

The neurons appeared normally myelinated adjacent to capillaries with patent lumens even though the endothelial cytoplasm was filled with electron-dense inclusions (Fig. 9a, 12d).

The pericyte cytoplasm also contained spherical and tubular electron-dense inclusions (Fig. 13a). Endothelial cells appeared flattened, rather than cuboidal in some sections (Fig. 13b). The basement membrane was 0.7 microns thick. Some lipid deposition occurred in pericytes (Fig. 13b).

Experimental Hypertension

The dog with intraocular pressure elevated to 75 mmHg for one hour had spherical (0.25-0.5 microns) and dumbbell shaped (0.35 x 0.5 microns) double membrane bound electron-dense inclusions in the endothelial and pericyte cytoplasm (Fig. 14-15a). There was abundant free ribosomes, rough ER, and actin microfilaments in microvillous lumenal projections (Fig. 14d). Endothelial cell vacuolations were adjacent to demyelinated areas in axons. The endothelial cell basement membrane was also thin in this area (Fig. 14d). Deymelination of axons was extensive (Fig. 15b). Microvillous projections were blunted (Fig. 15a). Some electron-dense inclusions had hollow centers and probably represented newly formed inclusions. Others showed evidence of an internal substructure (Fig. 15b).

Pericytes accumulated electron-dense material in their cytoplasm (Fig. 15d). Perfusion caused lumenal dilatation and stretching of the endothelial cells in some capillaries (Fig. 15d).

Normal Beagles

Six-month, one-year, two-year and six-year-old normal dogs were studied. Normal laminar capillaries were alternately in contact with the laminar extravascular space, containing collagen fibers arranged as loose connective tissue, and neural axon bundles. These capillaries had a continuous nonfenestrated endothelial cell layer with an adventitial layer surrounded by astrocytes (Fig. 16a, 16b). Long and tortuous tight junctions between endothelial cells were noted (Fig. 16a). Oligodendrocytes were present because the nerve bundles are myelinated anterior to the optic disc in the canine. Capillary endothelial cells and pericytes were completely enclosed by basement membrane. Endothelial cell nuclei protruded into the lumen (Fig. 16a). Microfilaments could be seen in the capillary endothelial cells. Capillary lumen diameter was 5-9 microns. With the perfusion fixation technique used in this experiment, capillary lumens tended to be dilated with the endothelial cytoplasm flattened. In some capillaries, however, the endothelial nucleus appeared to bulge into the adjacent connective tissue space (Fig. 16c).

Endothelial cells contained abundant conventional cytoplasmic organelles. Micropinocytotic vesicles were abundant in the endothelial cytoplasm (Fig. 16d). Most appeared facing opposite the lumen (Fig. 16a). The cytoplasm had a high electron density due to numerous ribosomes and rough ER (Fig. 16d, 17a). Some ribosomes were attached to short sacs of endoplasmic reticulum (Fig. 16c, 17a). Mitochondria were elongated and spherical, and were scattered widely (Fig. 16a). The cristae were not prominent (Fig. 16d, 17b). Membrane bound electron-dense bodies were few in number, measured 2

microns in diameter (Fig. 17c, 18a), and were spherical or elongated in shape with dense, homogeneous interiors (Fig. 18a).

Pericytes had less rough endoplasmic reticulum than endothelial cells and were surrounded by a basement membrane that fused with the basement membrane of adjacent endothelial cells (Fig. 16c). Micropinocytotic vesicles and mitochondria were present. The single cell layer of pericytes appeared discontinuous as it was not seen in all sections (Fig. 16b). No neural innervation or microtubules were noted in pericytes or endothelial cells.

FIGURE 1. TRANSMISSION ELECTRON MICROSCOPY OF PREGLAUCOMATOUS BEAGLES. a. Spherical electron dense inclusions (0.5 1) are noted in the capillary endothelial cell cytoplasm (arrow). Laminar collagen surrounds the capillary. (16,000 X.) b. Electron-dense inclusions are scattered throughout the endothelial cell cytoplasm (arrows). The endothelial nucleus and laminar collagen appear normal. (8,000 X.) c. Many oval electron-dense inclusions (arrows) are present in this laminar capillary. The pericyte nucleus (P) is also present. (6,300 X.) d. A rod-like substructure (arrow) is seen in some electron-dense inclusions. (12,500 X.)

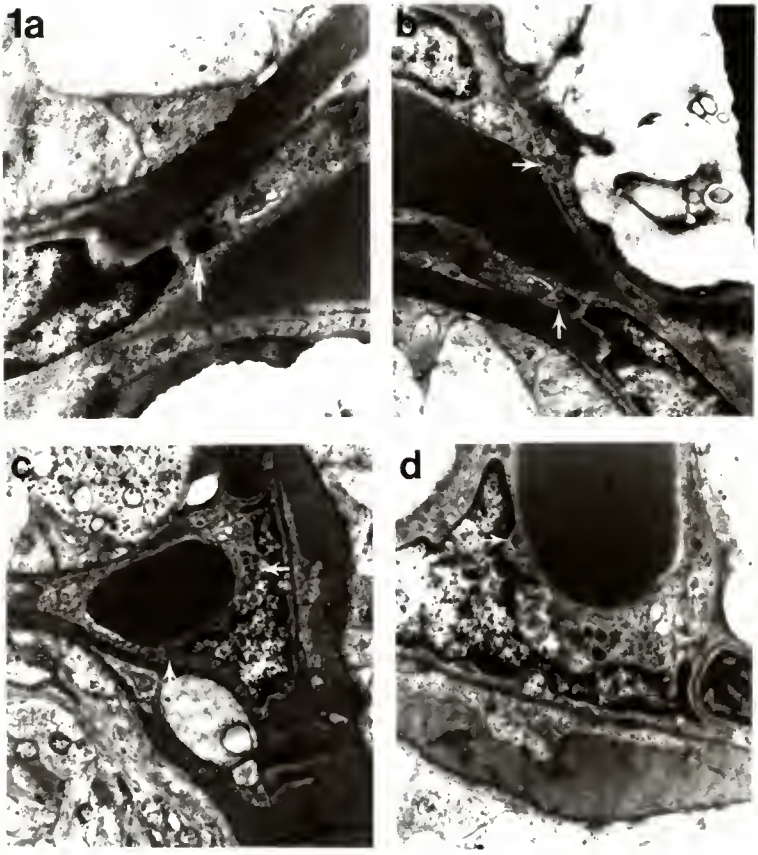
1a
b
c
d

FIGURE 2. TRANSMISSION ELECTRON MICROSCOPY OF EARLY GLAUCOMATOUS BEAGLES. a. Large membrane bound inclusions are present (arrows). The endothelium appears swollen with a disrupted cell membrane. (20,000 X.) b. Several membrane bound electron-dense endothelial cell cytoplasmic inclusions (arrows) are noted. (20,000 X.) c. Large vacuolated areas (arrows) of endothelial cell cytoplasm are present. (20,000 X.) d. Prominent vacuoles are present in thin areas of endothelial cytoplasm with adjacent basement membrane also thin. (31,500 X.)

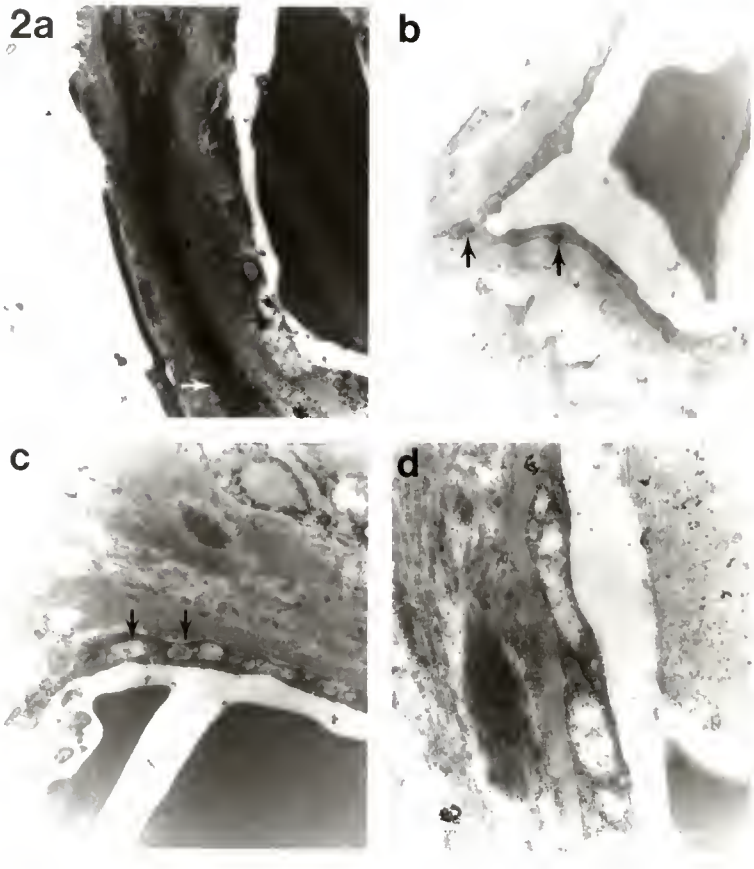
2a
b
c
d

FIGURE 3. TRANSMISSION ELECTRON MICROSCOPY OF EARLY GLAUCOMATOUS BEAGLES. a. Another region of a laminar capillary endothelial cell reveals severe cytoplasmic vacuolation (25,000 X.) b. Extensive vacuolization is present with free ribosomes decreased in quantity. (16,000 X.)

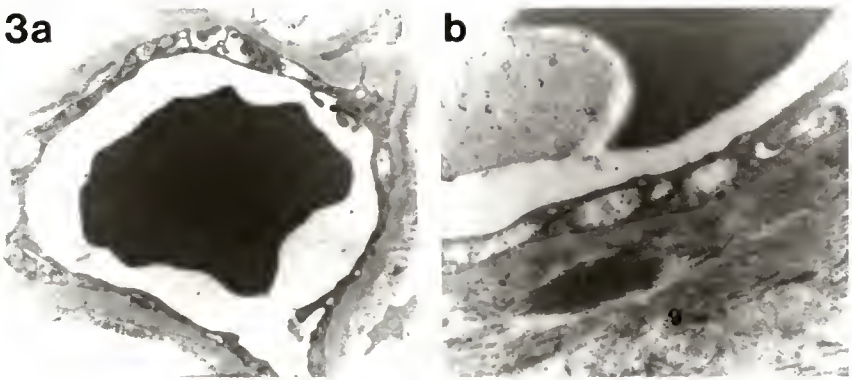
3a
b

FIGURE 4. TRANSMISSION ELECTRON MICROSCOPY OF MODERATE GLAUCOMATOUS BEAGLES. a. Spherical membrane bound electron-dense inclusions (arrows) are noted. (16,000 X.) b. Tubular and spherical membrane bound inclusions are found in the endothelial cytoplasm (black arrow). Many micropinocytotic vesicles are present. Endothelial cytoplasmic fat is noted (white arrow). (16,000 X.) c. The endothelial cytoplasm is filled with tubular and spherical membrane bound inclusions. Note cytoplasmic extensions into the capillary lumen (arrows). (12,500 X.) d. Tubular and spherical electron-dense inclusions are present. (16,000 X.)

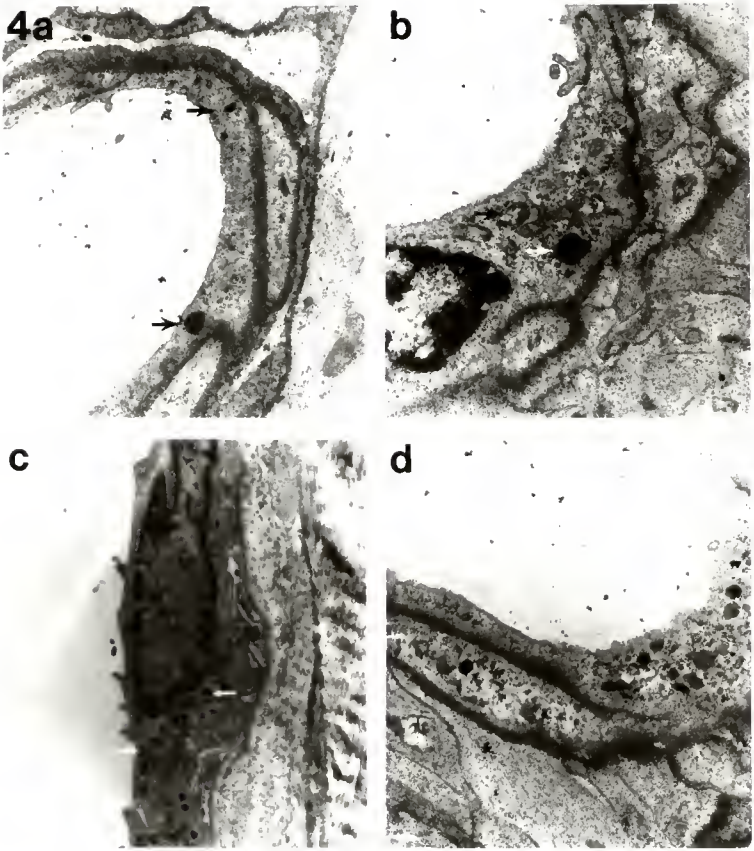
4a
b
c
d

FIGURE 5. TRANSMISSION ELECTRON MICROSCOPY OF MODERATE GLAUCOMATOUS BEAGLES. a. Double unit membrane (arrow) is apparent in these electron-dense inclusions. (50,000 X.) b. The endothelial cytoplasm contains many spherical membrane bound electron-dense inclusions. (10,000 X.) c. Endothelial and pericyte cytoplasm is filled with spherical electron-dense inclusions. Red blood cells are contained in the lumen. Collagen surrounds the capillary. (3,150 X.) d. Two adjacent endothelial cells (black arrow) contain many electron-dense inclusions. One inclusion has a rod-like structure (white arrow) internal to the membrane. (16,000 X.)

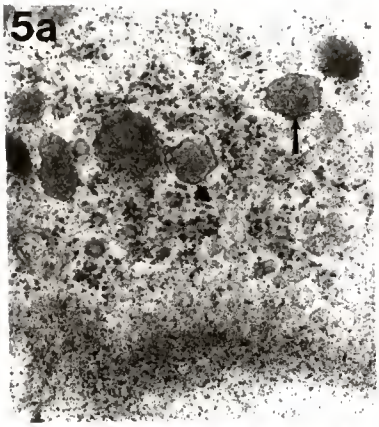
5a

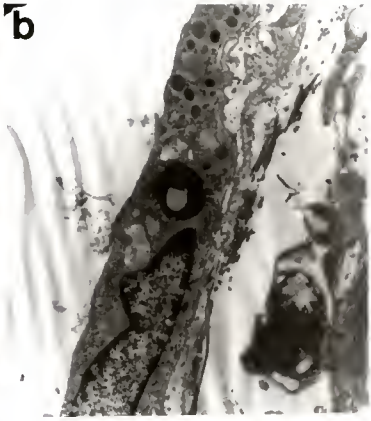
b

c

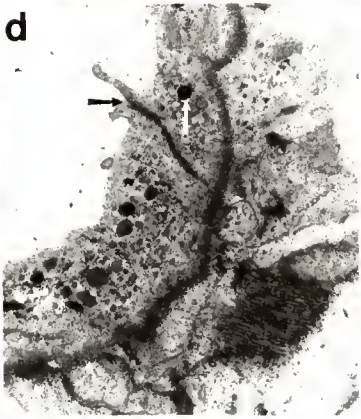
d

FIGURE 6. TRANSMISSION ELECTRON MICROSCOPY OF MODERATE GLAUCOMATOUS BEAGLES. a. Microvilli appear normal with membrane bound inclusions present. (12,500 X.) b. Many electron-dense inclusions are noted with vacuolation of the endothelial cytoplasm present. (6,300 X.) c. A tubular substructure (arrow) is present in this membrane bound electron-dense inclusion. (16,000 X.) d. Electron-dense inclusions and a degenerating cytoplasmic organelle are present in the pericyte cytoplasm. The formvar coated grid has pulled back to leave the artefact (a). (10,000 X.)

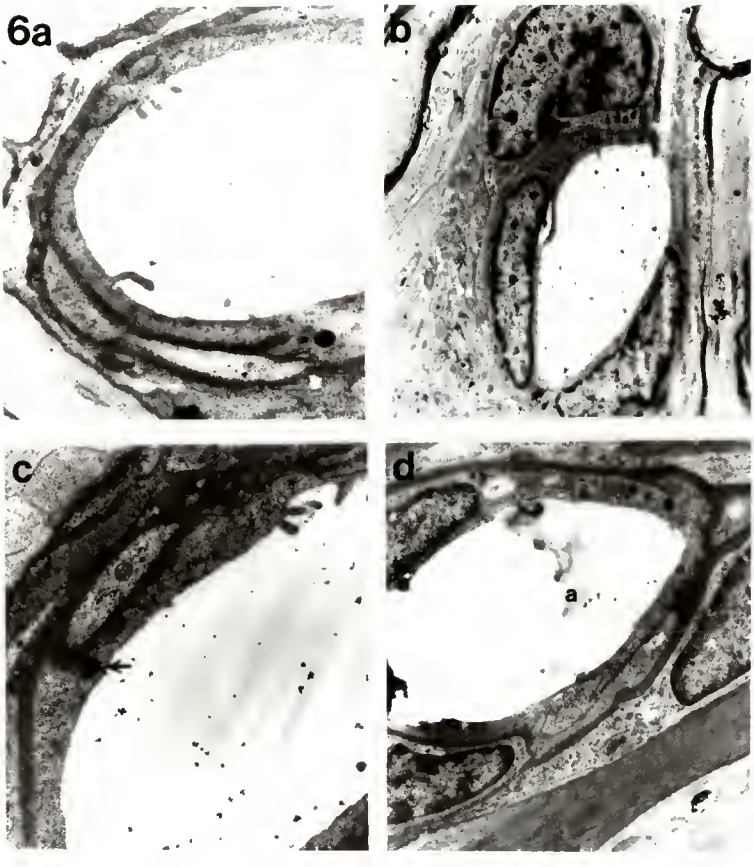
6a
b
c
d
a

FIGURE 7. TRANSMISSION ELECTRON MICROSCOPY OF MODERATE GLAUCOMATOUS BEAGLES. a. Axons with degenerating mitochondria (m) are adjacent to a capillary with electron-dense inclusions in the cytoplasm. A = artefactual fold (8,000 X.) b. The laminar collagen framework appears to be breaking down. Many electron-dense inclusions are noted. A = artefactual fold (8,000 X.) c. Microvillous processes are blunted. Electron-dense inclusions are present. (16,000 X.)

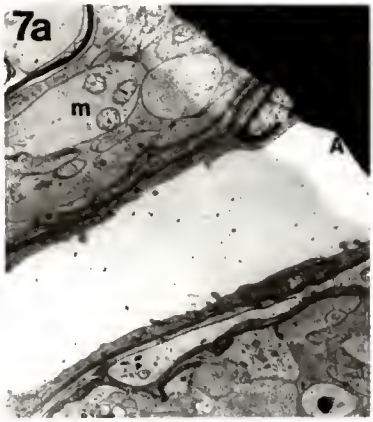
7a
m
A

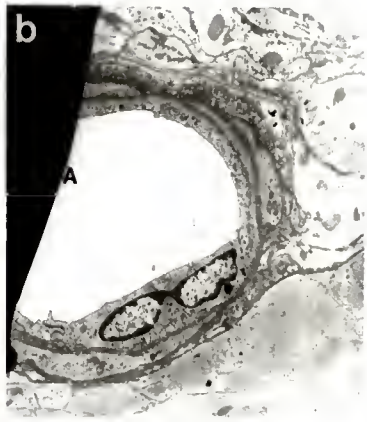
b
A

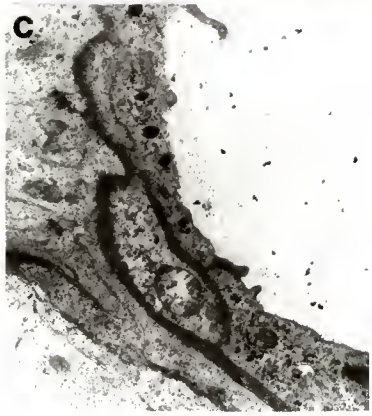
c

FIGURE 8. TRANSMISSION ELECTRON MICROSCOPY OF AOVANCEO GLAUCOMATOUS BEAGLES. a. Double membrane bound electron-dense inclusions are noted. (20,000 X.) b. Large oval electron-dense inclusions, nuclear crenulation and lumen (L) collapse are present. (20,000 X.) c. Several electron-dense inclusions are present in the endothelial cell cytoplasm. Some are adjacent to a Golgi complex (black arrow). Four endothelial cell junctions are shown (hollow arrows). (6,300 X.) d. Tubular and oval electron-dense inclusions are present in a thickened endothelial cytoplasm. A micropinocytotic vesicle is open to the capillary lumen. A = artefactual fold. (10,000 X.)

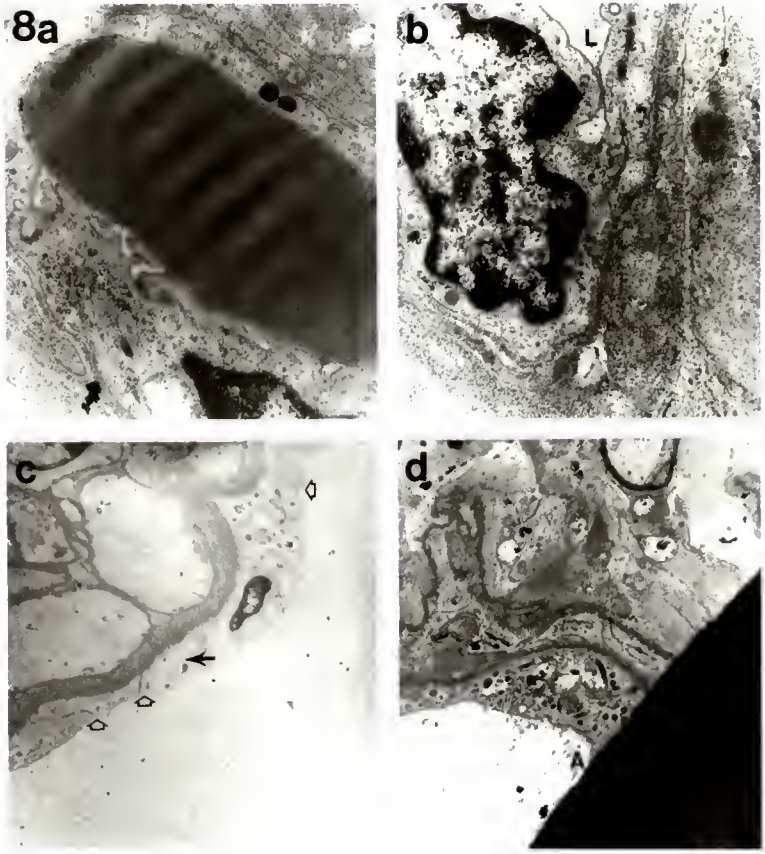
8a
b
L
c
d
A

FIGURE 9. TRANSMISSION ELECTRON MICROSCOPY OF ADVANCED GLAUCOMATOUS BEAGLES. a. Many electron-dense inclusions fill the cytoplasm of this capillary. Less cellular deterioration, i.e. healthy myelin, is adjacent to this area. Blood flow may have been better here. A = artefactual fold. (6,300 X.) b. Electron-dense inclusions are present in the endothelial cytoplasm. Pericyte (P) appears normal. Formvar has pulled away to cause the artefact (A). (12,500 X.) c. Many electron-dense inclusions are present in pericyte and endothelial cytoplasm. Lumen appears patent. (5,000 X.) d. Many small and large electron-dense inclusions are present in the endothelial cell cytoplasm. (16,000 X.)

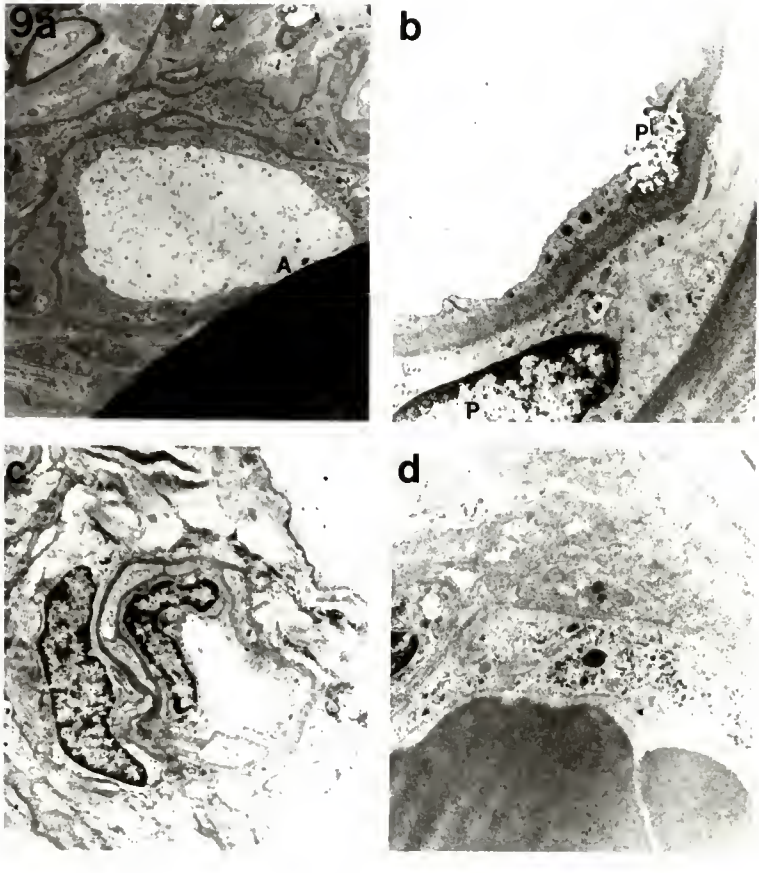
9a
A
b
P
P
c
d

FIGURE 10. TRANSMISSION ELECTRON MICROSCOPY OF AOVANCEO GLAUCOMATOUS BEAGLES. a. Circular opacities (arrow) in a membrane bound electron-dense inclusion (0.25 microns) are present. Some membrane bound vacuoles (1.2 microns) may be degenerate mitochondria as cristal remnants appear to be present (hollow arrow). (20,000 X.) b. This capillary is in a trabecular beam of the lamina cribrosa. The lumen is partially collapsed in spite of the perfusion fixation. Abluminal vesicles (arrow) are noted. Some vesicles appear to be engulfing cytoplasm. Membrane bound electron-dense inclusions are noted. (8,000 X.) c. Membrane bound inclusions are present in this capillary. There is less rough endoplasmic reticulum than in some sections. The capillary lumen (L) is collapsed. (16,000 X.) d. The capillary lumen (L) is collapsed in this perfusion fixed specimen with electron-dense inclusions present. Myelinated nerve fibers contain degenerating mitochondria. Micropinocytotic vesicles open into the capillary lumen. (20,000 X.)

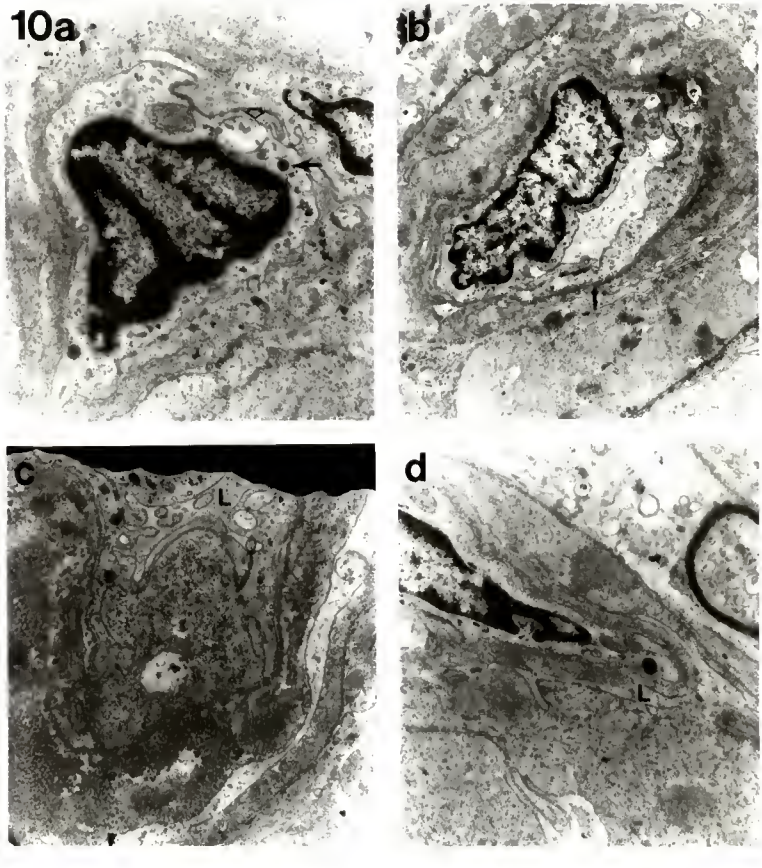
10a
b
c
L
d
L

FIGURE 11. TRANSMISSION ELECTRON MICROSCOPY OF ADVANCED GLAUCOMATOUS BEAGLES. a. Axonal deterioration is evident next to a capillary (c) with a collapsed lumen. Mitochondria are cystic. (5,000 X.) b. Axon is compressed (arrow) by a dislocated trabecular beam. Mitochondria appear degenerate. (6,300 X.) c. A laminar capillary has several electron-dense inclusions, rough endoplasmic reticulum and large cytoplasmic cysts or vacuolated areas. (4,000 X.) d. Many micropinocytotic vesicles open into the capillary lumen. Membrane bound electron-dense inclusions are present. (16,000 X.)

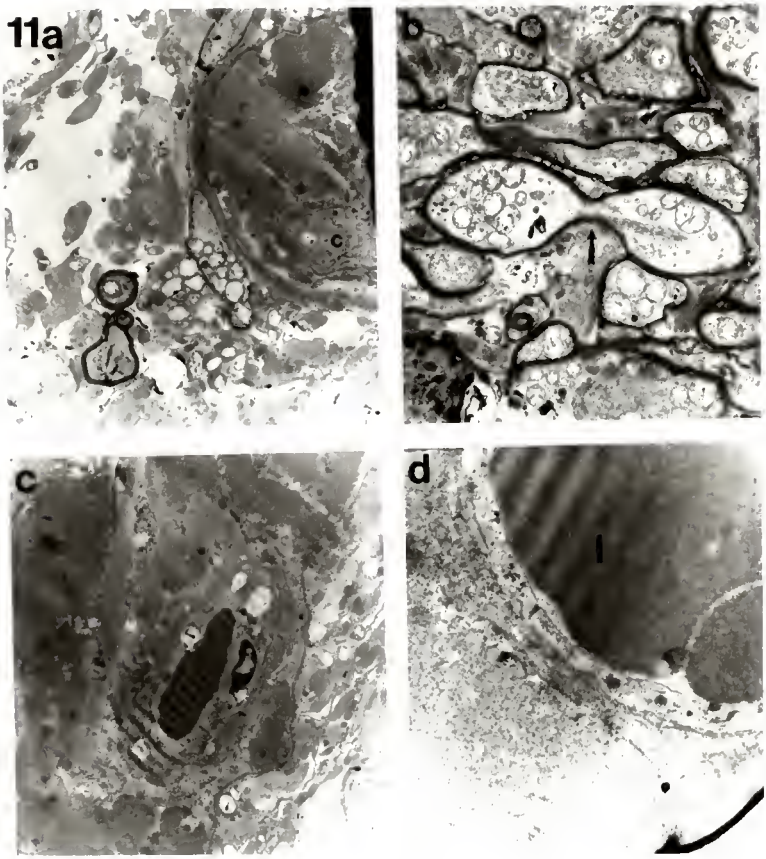
11a
c
b
c
d
l

FIGURE 12. TRANSMISSION ELECTRON MICROSCOPY OF ADVANCED GLAUCOMATOUS BEAGLES. a. Capillary (c) with red blood cell in lumen. Many electron-dense inclusions are present. There is less rough endoplasmic reticulum than in some sections. (4,000 X.) b. Microvilli with microfilaments appear reduced in number. (8,000 X.) c. No microvilli with microfilaments are present. Several inclusions and many micropinocytotic vesicles are noted. Interendothelial cell processes are swollen. A platelet and red blood cell are present in the lumen. (20,000 X.) d. Myelination appears normal in this region in spite of the density of electron-dense inclusions in the endothelial cytoplasm. A = artefactual fold. (8,000 X.)

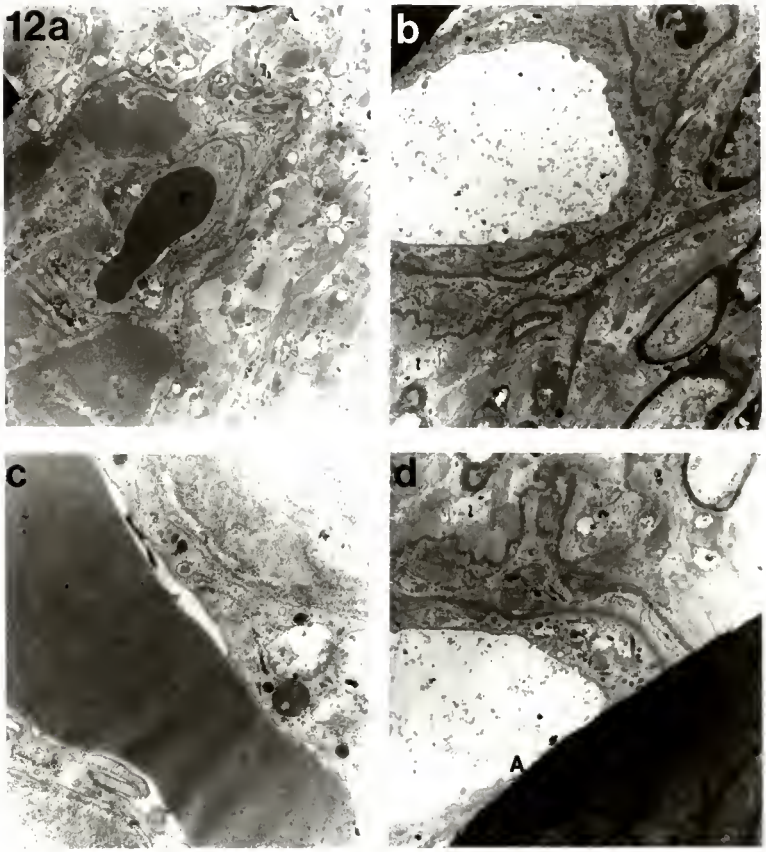
12a
b
c
d
A

FIGURE 13. TRANSMISSION ELECTRON MICROSCOPY OF ADVANCED GLAUCOMATOUS BEAGLES. a. Pericyte and endothelial cytoplasm contain spherical and tubular electron-dense inclusions. (8,000 X.) b. Pericyte and endothelial cytoplasm contain electron dense inclusions. Autophagosomes (arrow) are present. The nucleus is prominent and irregular. (5,000 X.) c. Endothelial cells are flattened, rather than cuboidal, with lipid (arrow) deposited in pericyte cytoplasm. (12,500 X.)

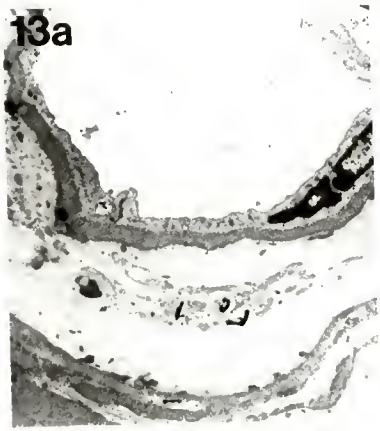
13a

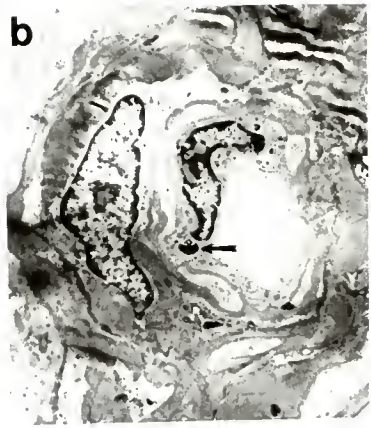
b

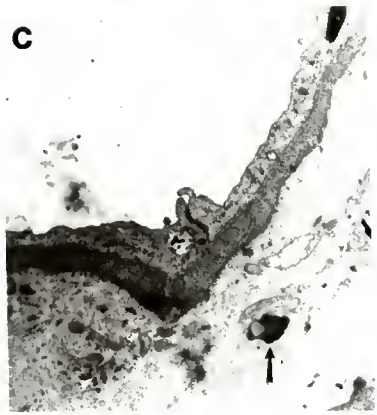
c

FIGURE 14. TRANSMISSION ELECTRON MICROSCOPY OF A DOG WITH EXPERIMENTAL OCULAR HYPERTENSION. a. Electron-dense inclusions are present. Perfusion fixation has dilated the capillary lumen. (8,000 X.) b. Microvillous extensions are present. A few inclusions (arrows) are found in the endothelial and pericyte cytoplasm. (4,000 X.) c. Spherical membrane bound inclusions are present in pericyte cytoplasm. A dumb-bell shaped inclusion is in the endothelial cytoplasm. Microvilli protrude into the lumen. There is abundant rough endoplasmic reticulum and many free ribosomes. (20,000 X.) d. Microfilaments (arrow) are abundant near the capillary lumen and in microvilli (0.8 microns). Severe vacuolation of the endothelial cell is present. The endothelial vacuolation may be caused by degeneration or poor fixation. Ruptured myelin (white arrow) indicates tissue damage from elevated intraocular pressure due to ischemia. The adjacent vacuolated areas with adjoining thin basement membrane could represent a pocket of ischemic damage. (20,000 X.)

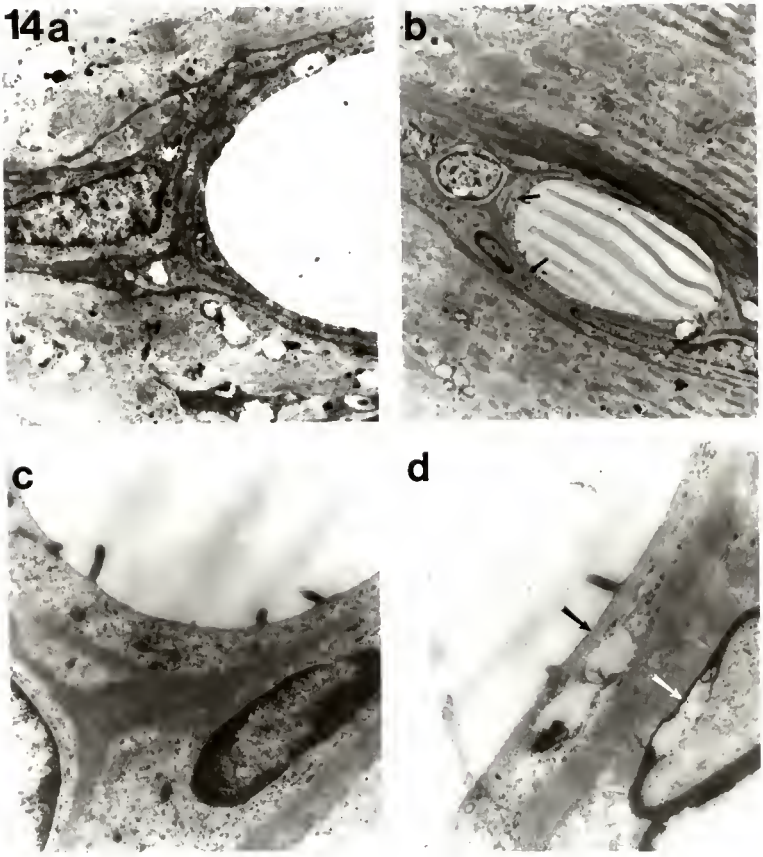
14a
b.
c
d

FIGURE 15. TRANSMISSION ELECTRON MICROSCOPY OF A DOG WITH EXPERIMENTAL OCULAR HYPERTENSION. a. Dumb-bell shaped inclusions (arrow) in endothelial cytoplasm. (20,000 X.) b. Nerve fibers surround this laminar capillary and show evidence of extensive myelin disruption in several axons. (4,000 X.) c. A grazing section of an endothelial cell shows electron-dense inclusions with hollow centers and central rodlets. (20,000 X.) d. This pericyte has accumulated an abnormal amount of electron dense material in its cytoplasm. Perfusion fixation resulted in lumenal dilatation and endothelial cell stretching. Few microvilli are seen. (10,000 X.)

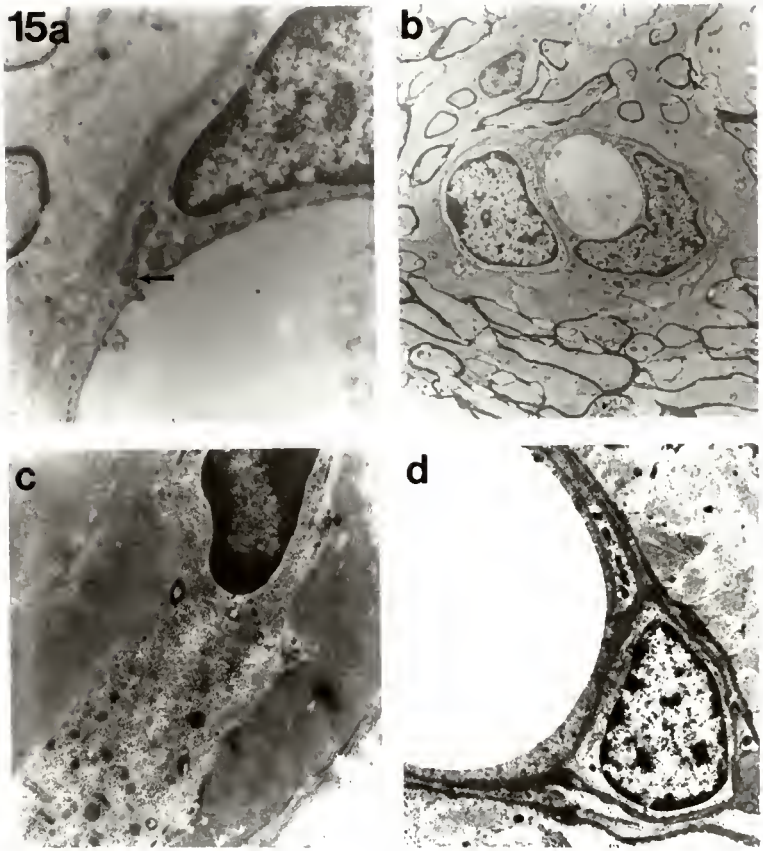
15a
b
c
d

FIGURE 16. TRANSMISSION ELECTRON MICROSCOPY OF NORMAL DOGS. a. Endothelial nucleus is prominent. Membrane bound vesicles are probably mitochondria. (1 year old, 6,300 X.) b. Many microvilli are present. Several cytoplasmic organelles are noted. (6 months old, 7,000 X.) c. Endothelial nucleus bulges slightly into the lumen of the capillary. (6 months old, 10,000 X.) d. Numerous ribosomes are present. Mitochondria appear vesicular and could indicate inadequate fixation. (1 year old normal, 16,000 X.)

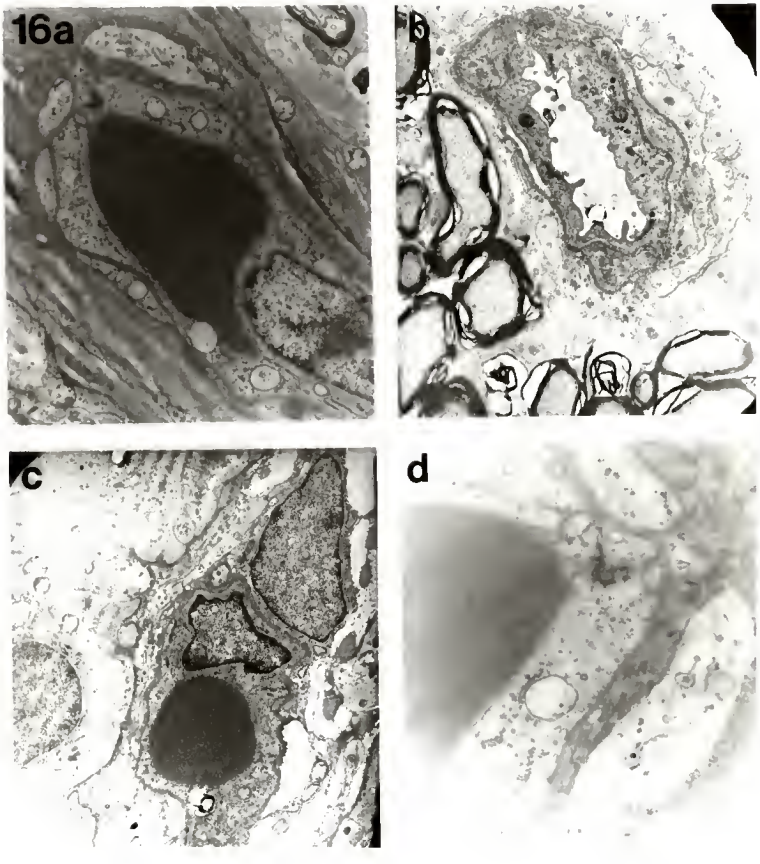
16a
b
c
d

FIGURE 17. TRANSMISSION ELECTRON MICROSCOPY OF NORMAL OOGS. a. A membrane bound electron-dense inclusion (arrow) is present. The vesicular structure is a degenerate organelle, probably a mitochondria. (1 year old, 16,000 X.) b. Mitochondria with cristae are present. (6 months old, 15,000 X.) c. A spherical membrane bound electron-dense inclusion is present (hollow arrow). Cystic mitochondria (arrow) and micropinocytotic vesicles are noted. (One year old, 16,000 X.)

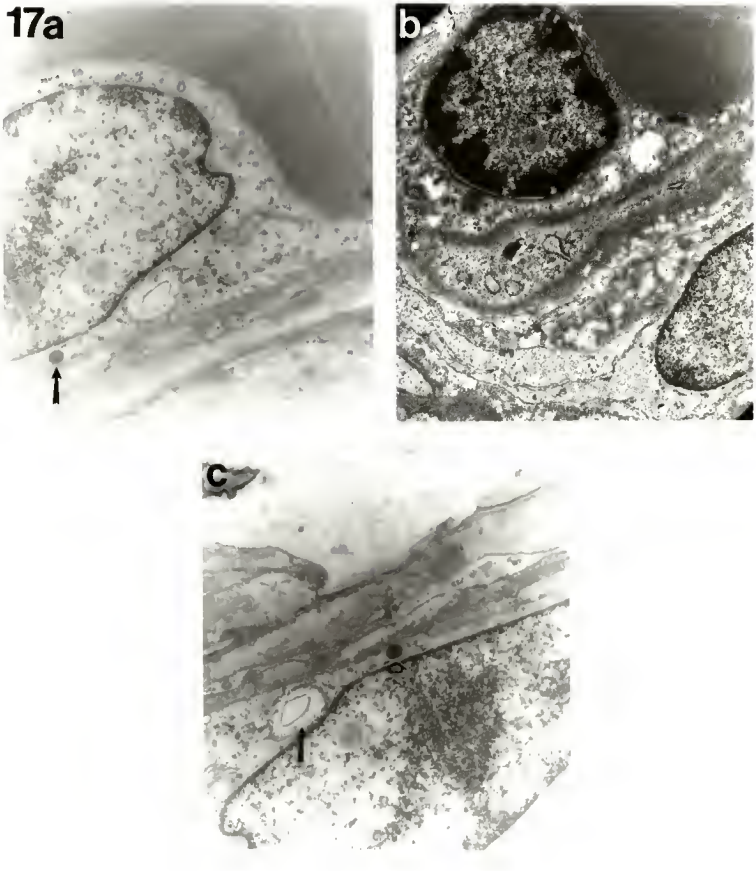
17a
b
c

FIGURE 18. TRANSMISSION ELECTRON MICROSCOPY OF NORMAL DOGS. a. Micropinocytotic vesicles and an inclusion are noted. (One year old, 20,000 X.) b. No electron-dense inclusions are seen in this section. A red blood cell is present in the lumen. (5 year old, 10,000 X.)

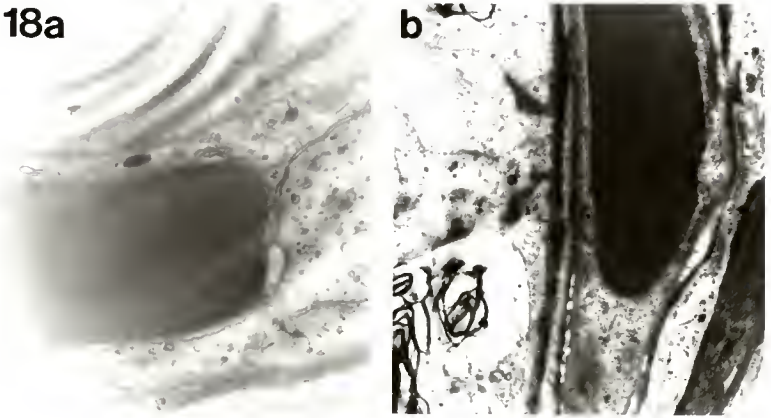
18a
b

Experiment 3: Scanning Electron Microscopy of Corrosion Casts of the Canine Optic Nerve Microcirculation

Full castings of the entire ocular vasculature were obtained from 4 normal dogs and 2 Beagles with glaucoma (1 moderate and 1 severely affected). All casts presented mildly expanded vascular lumens but enabled detailed scanning electron microscopic examination of microvascular connections and distributions.

One medial and one lateral large diameter-sized (0.35-0.45 mm) arteries supplied a circumferential anastomosing complex of small and medium diameter microvessels 1 mm posterior to the insertion of the optic nerve (Fig. 1, 2). These large diameter-sized arteries anastomosed at several sites and also directly supplied the posterior choroidal arteries (Fig. 1b, 2a, 3). Internal to the supplying arteries, distended, smooth surfaced large diameter sacculations were noted in 3 normals (Fig. 1b, 2a, 3b, 5) and a glaucoma dog (Fig. 4). These vessels may have been diverticuli or sacculations of one of the main supplying arteries or veins, or were artefacts due to elevated plastic infusion pressure.

The radial vessel complex (Fig. 4b, 6a) was a dense meshwork of medium (88 microns) diameter-sized vessels and capillaries (24 microns). In four dogs large (550 microns) smooth surfaced dilatations also partially circumscribed the vascular ring. There was widespread anastomosing of the medium diameter-sized vessels and capillaries in this region (Fig. 6b).

Vessels (135 microns) with deep longitudinal indentations extended from the posterior vascular ring to form a radially oriented set of pillar-like vessels that surrounded the scleral canal and

lamina cribrosa. These pillars were short posterior ciliary arteries (SPCA) and each originated from several of the larger diameter-sized arteries (Fig. 7a). The number of vessels forming the pillars varied from 6 to 10 (Fig. 7b, 8b, 12a). More flattened "vein-like" vessels were seen to be less filled in a few casts internal to the striated arteries (Fig. 5a, 9a). Endothelial mural impressions were rare but when viewed were vein-like in these flattened vessels. The large longitudinally striated vessels branched near the scleral canal to form choroidal arteries with smaller branches (cilioretinal arteries) continuing anteriorly to supply the retinal (Fig. 9b, 10) capillary system.

Capillaries to the lamina cribrosa were widely anastomotic and originated from the SPCA, cilioretinal arteries and pial vessels (Fig. 1a, 4b, 11-13a). The anterior laminar region also received some blood from the retinal capillaries (Fig. 13). There was a suggestion of some laminar capillaries having connections to the choriocapillaris (Fig. 13a), but this was a minor component of the anterior optic nerve circulation.

The choroidal arteries (87-95 microns) had periodic annular constrictions (Fig. 14a) as they radiated from the peripapillary region. Interarterial anastomoses formed between branches of the same parent artery. The choroidal arteries intersected between the larger choroidal veins (Fig. 5b) and branched into smaller vessels before supplying the choriocapillaris (Fig. 9b, 14b, 15). The direct connection between the choriocapillaris and choroidal veins was observed (Fig. 15b). The choriocapillaris (9 microns) formed a dense and extensive mosaic pattern (Fig. 16). Choroidal veins (220-225

microns) were more numerous than arteries. Most choroidal veins ended blindly at the scleral canal and converged toward the vortex veins in the equatorial region. Retinal veins drained into the choroidal system (Fig. 5a). Anastomoses between choroidal veins were prominent between the large venous trunks (Fig. 17a).

Peripapillary retinal arteries (58 microns), veins (110 microns) and capillaries were prominent on the anterior retinal surface. Retinal arteries entered the globe at the edge of the scleral canal (Fig. 15b). Retinal capillary networks were infrequently seen due to their fragility during the casting maceration process (Fig. 16, 17b). Endothelial cell mural impressions of retinal arteries were seen as longitudinally oriented pits in the cast surface (Fig. 18a). Retinal veins had less numerous oval pits (Fig. 18b). Annular constrictions were prominent at branch points for smaller diameter arterial vessels (22 microns) in the retinal circulation (Fig. 18b, 19).

Spherical smooth surfaced structures seen in the posterior vascular region had connections to a vein-like structure and were most likely "blow-out" artefacts (Fig. 5b, 20, 21b) due to improperly elevated filling pressure. Filling defects were seen in a few vessels (Fig. 14a, 21). Leakage of cast material through the endothelial cell junctions occurred occasionally (Fig. 22).

Bulging or localized distension of the large posterior vessels was noted (Fig. 1a, 2a), and carried to a more prominent degree could have resulted in the sinus-like sacculations noted. No description of such a structure exists in the literature.

No differences in the number of vessels, vessel location or artefacts were noted between the casts of the normal dogs and Beagle dogs affected with hereditary POAG.

FIGURE 1. SCANNING ELECTRON MICROSCOPY OF CORROSION CASTS.
a. Posterior view of corrosion cast with large vessels feeding an extensive complex of arteries, veins and capillaries that surround the optic nerve. (20 X.) b. The choroidal arterial supply has two sources: 1) pillar-like short posterior ciliary arteries (SPCA) serve the optic nerve region (star), while 2) posterior vessels from the external ophthalmic artery and long posterior ciliary arteries serve more anterior regions (hollow arrows). (22 X.)

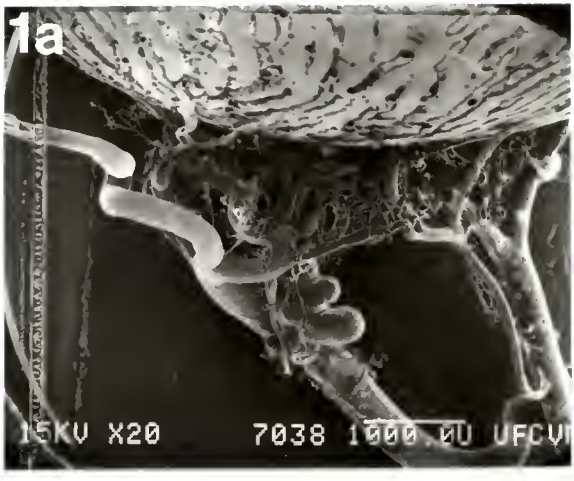
1a
15KV X20
7038 1000.0U UFCV

b

FIGURE 2. SCANNING ELECTRON MICROSCOPY OF CORROSION CASTS.
a. Pillar-like SPCA are seen on the right (hollow arrow). SPCA are external to complementary veins. Dilated vessels on left appear to originate from a large artery (solid arrow). (32 X.) b. A long posterior ciliary artery branches from the external ophthalmic artery (arrow). The dilated sinus region is seen (star). (20 X.)

2a
15KV X32
7043 1000.0U UFCVM

b

FIGURE 3. SCANNING ELECTRON MICROSCOPY OF CORROSION CASTS. a. A long posterior ciliary artery branches into choroidal arteries (arrow). (54 X.) b. Prominent vascular sinus is on the left. Choroidal arteries and veins (c) are also present. (60 X.)

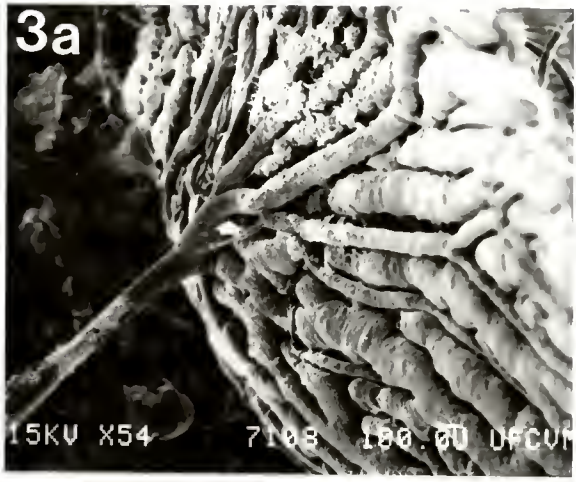
3a
15KV X54
7108
100.0U UFCVM

b
c
15KV X60
7044
100.0U UFCVM

FIGURE 4. SCANNING ELECTRON MICROSCOPY OF CORROSION CASTS. a. A radial complex of small and large vessels surrounds the optic nerve. (32 X.) b. Greatly distended, smooth surfaced, large diameter-sized vessels are present internal to arteries (arrows). (78 X.)

4a
15KV X32
7042 1000.0U UFCVM

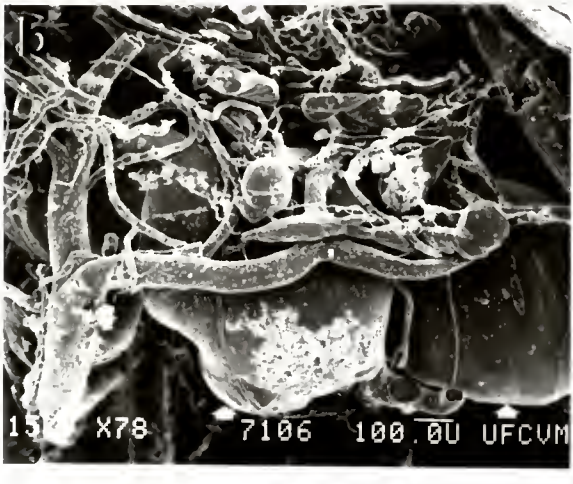
b
15 X78
7106 100.0U UFCVM

FIGURE 5. SCANNING ELECTRON MICROSCOPY OF CORROSION CASTS. a. Large vascular sinus is posterior to the scleral lamina cribrosa region. Short posterior ciliary arteries (SPCA) have longitudinal striations (star) and are external to less filled short posterior ciliary veins (arrow) (SPCV). (48 X.) b. Many large diameter vessels are posterior to the vessels supplying the optic nerve and retina. Spherical structures (arrows) are probably perfusion artefacts. (26 X.)

5a
15KV

b
15KV

FIGURE 6. SCANNING ELECTRON MICROSCOPY OF CORROSION CASTS. a. The choriocapillaris (CC) is superficial to the posterior large vessel and sinous layer. Capillaries are noted in the laminar region (arrows). (36 X.) b. Many small vessels have anastomotic connections in the complex of vessels posterior to the globe. (66 X.)

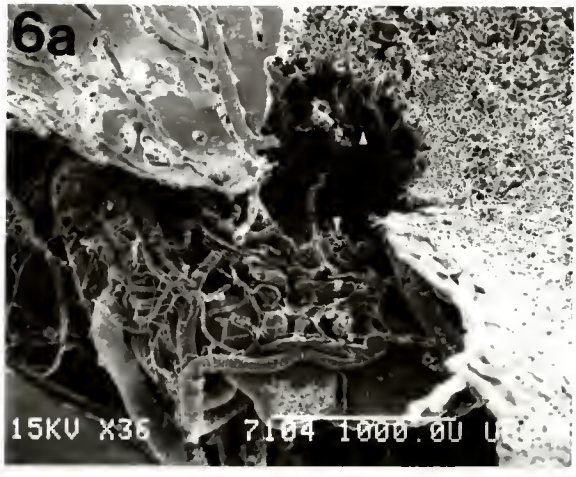
6a
15KV X36
7104 1000.0U

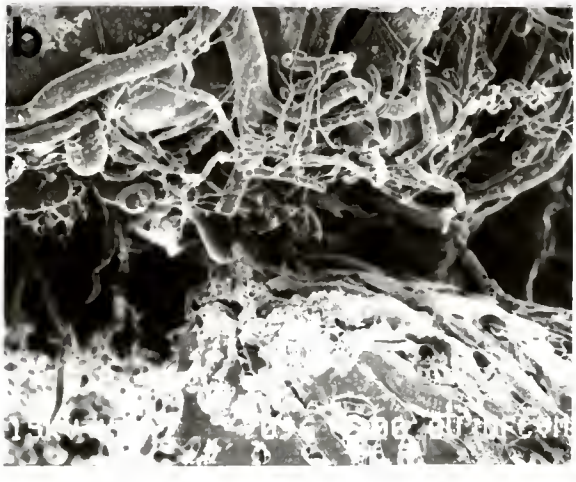
b

FIGURE 7. SCANNING ELECTRON MICROSCOPY OF CORROSION CASTS. a. One supplying artery forms three pillar-like SPCA (arrows) in this view. (60 X.) b. The anterior surface of the uveal tract has retinal arterioles and venules (arrows), the choriocapillaris, and the optic canal. Short posterior ciliary arteries ring the optic canal (star). (36 X.)

7a
15KV X60 7047 100.00 UFCUM

b
*

FIGURE 8. SCANNING ELECTRON MICROSCOPY OF CORROSION CASTS. a. Short posterior ciliary arteries (SPCA) form striated pillars around the optic canal. The branching into cilioretinal and choroidal arteries is noted (arrow). Many optic nerve capillaries are seen in this region (star). The anterior optic nerve is at the bottom of the micrograph. (130 X.) b. Longitudinal striations in SPCA are pericytes or muscle folds. (750 X.)

8a

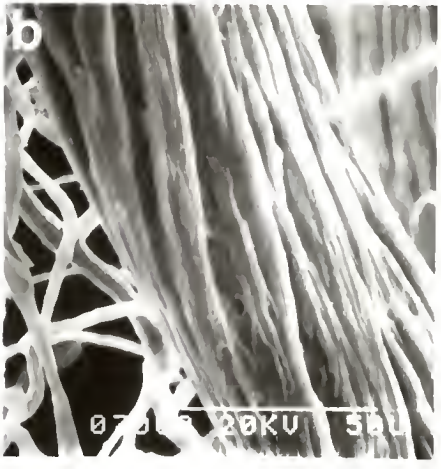
b
20KV

FIGURE 9. SCANNING ELECTRON MICROSCOPY OF CORROSION CASTS. a. The lobular structures internal to the striated SPCA are short posterior ciliary veins (SPCV). They did not fill completely with casting compound (arrow). (180 X.) b. SPCA's (star) branch to form choroidal (solid arrow) and cilioretinal arteries (hollow arrow). Branches from the choriorocapillaris extend into the scleral canal. Many other capillaries are also present in the laminar region. (60 X.)

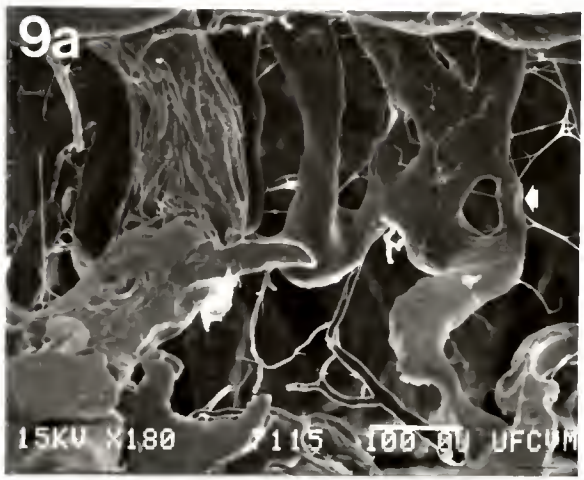
9a
15KV X180
115
100 µ UFCUM

b

FIGURE 10. SCANNING ELECTRON MICROSCOPY OF CORROSION CASTS. a. Anterior surface of cast shows the lobular choriocapillaries and cilioretinal (arrow) arteries making a ninety degree turn to the retina. Capillary sized vessels in the scleral canal originate from pial and cilioretinal vessels. (180 X.) b. Endothelial cell mural impressions present are like those seen in arteries in these two cilioretinal vessels at the edge of the scleral canal (arrow). (600 X.)

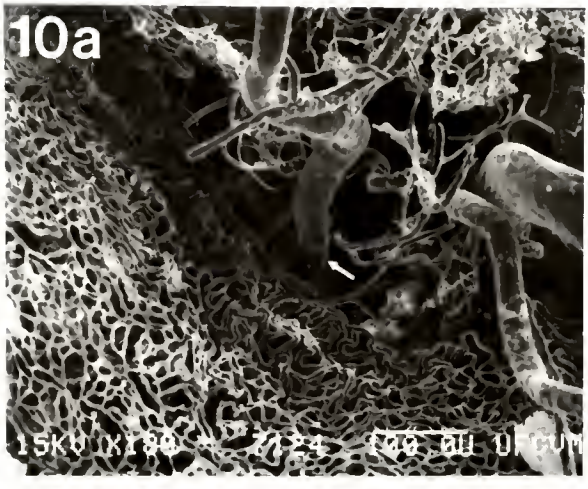
10a
15KV X180 7124 100.0U UFCUM

b
1
7123 10.0U UFCUM

FIGURE 11. SCANNING ELECTRON MICROSCOPY OF CORROSION CASTS. a. A dense vascular network (star) surrounds the orbital optic nerve and lamina cribrosa. (20 X.) b. Capillaries are seen in the scleral canal originating from a striated SPCA (arrow). Note arterial endothelial mural impressions on SPCA and choroidal arteries (hollow arrow). (94 X.)

11a
15KV X20 7039 1000.0U UFCVM

b

FIGURE 12. SCANNING ELECTRON MICROSCOPY OF CORROSION CASTS.
a. Arterial pillars of the SPCA feed the choroidal, optic nerve and retinal circulations. (100 X.) b. A dense nest of capillaries enclose the scleral canal (star). They appear independent of the choriocapillaris and originate posterior to the retinal surface from the cilioretinal and pial vessels. (86 X.)

12a

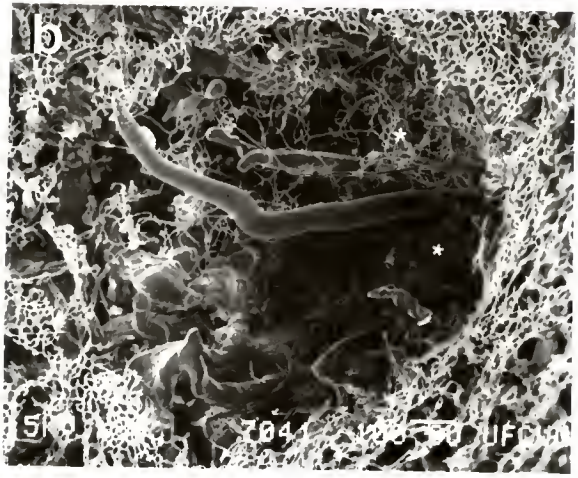
b

FIGURE 13. SCANNING ELECTRON MICROSCOPY OF CORROSION CASTS.
a. Capillaries bridge the scleral canal. Cilioretinal vessels are prominent (arrows) (160 X.) b. Periodic annular constrictions (arrow) are found in choroidal arteries as they move anteriorly. (100 X.)

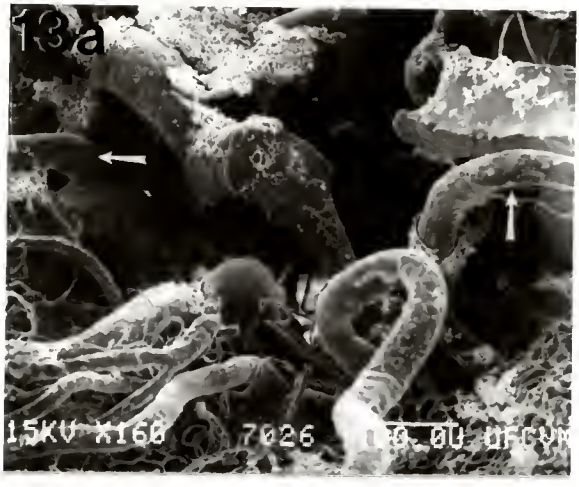
13a
15KV X160 7026 100.0U UFCVM

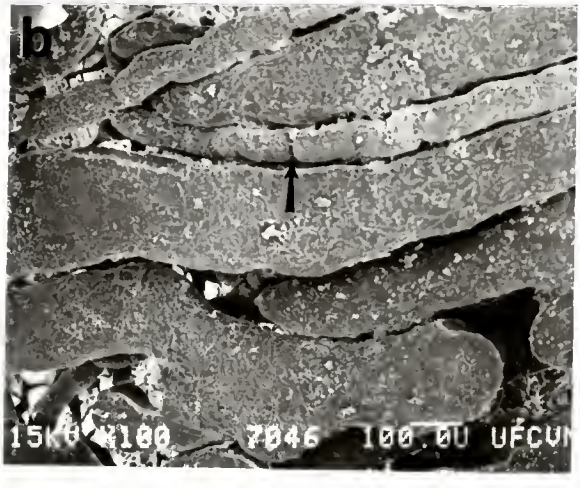
b
15KV X100 7046 100.0U UFCVM

FIGURE 14. SCANNING ELECTRON MICROSCOPY OF CORROSION CASTS. a. SPCA branch to form cilioretinal arteries (arrow) and choroidal arteries (hollow arrow). (78 X.) b. The choriocapillaris is supplied and drained by the choroidal vessels (arrows). (72 X.)

14a
1
15KV
100.0U UFCVM

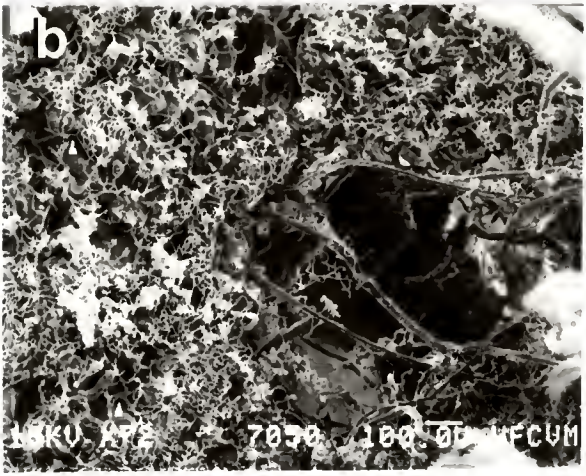
b
15KV
7070
100.0U UFCVM

FIGURE 15. SCANNING ELECTRON MICROSCOPY OF CORROSION CASTS. a. A choroidal vein receives blood from the choriocapillaris (arrow). A choroidal artery intertwines between the large veins (hollow arrow). (220 X.) b. The choriocapillaris forms a fine, widely anastomotic meshwork on the anterior choroidal surface. Retinal vessels are larger, prominent, and enter the globe at the periphery of the optic nerve. (22 X.)

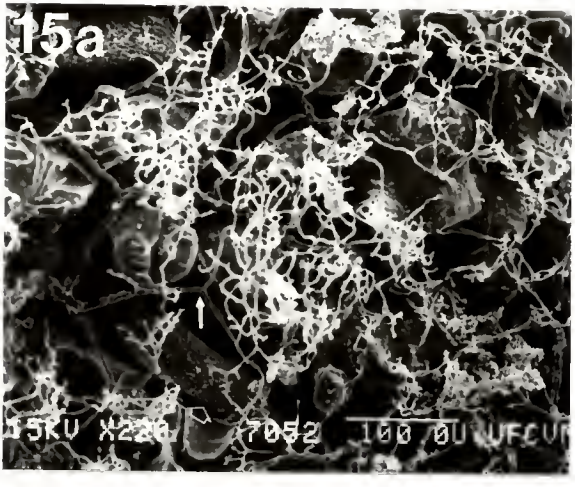
15a
15KV X220 7052 100.0U WFCUR

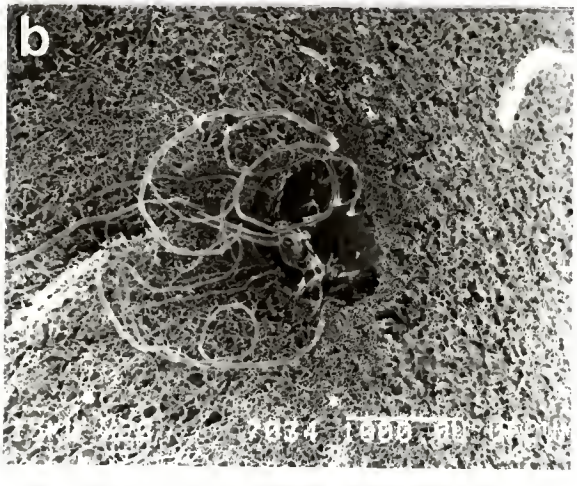
b

FIGURE 16. SCANNING ELECTRON MICROSCOPY OF CORROSION CASTS.
a. Cilioretinal arteries arise from the SPCA (arrow) and the cilioretinal veins drain into the SPCV (hollow arrow). Retinal capillaries did not survive the casting process. (54 X.) b. Choroidal veins anastomose as they move anteriorly and end blindly in some regions (arrows). (40 X.)

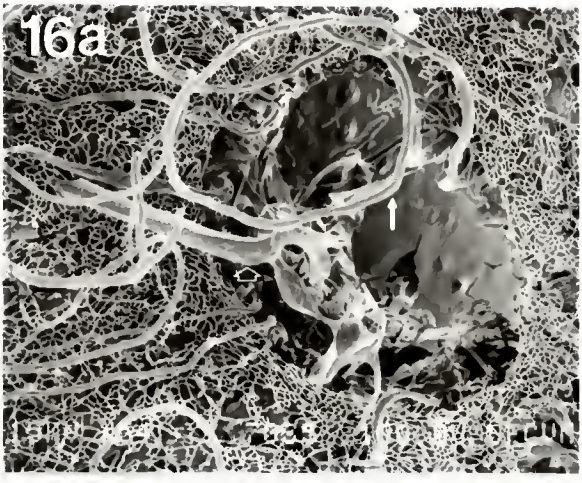
16a

b
15KV X40
7045
100.0U UFCUM

FIGURE 17. SCANNING ELECTRON MICROSCOPY OF CORROSION CASTS.
a. Cilioretinal vessels enter the globe at the periphery of the scleral canal. Retinal capillaries were rarely seen. (44 X.). b. Retinal arteriolar endothelial cell mural cell impressions are seen as longitudinally oriented pits in the cast surface. (1,800 X.)

17a
100.0U UFCU

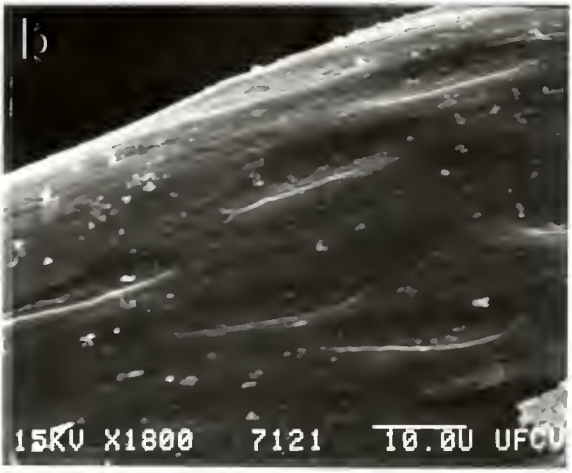
15KV X1800 7121 10.0U UFCU

FIGURE 18. SCANNING ELECTRON MICROSCOPY OF CORROSION CASTS.
a. Cilioretinal veins had oval endothelial cell mural impressions (arrow). Note annular constrictions at branch points of the smaller diameter arterioles (hollow arrow). (180 X.) b. Annular constriction is present at the branch point of a cilioretinal arteriole. (1,200 X.)

18a
15KV X180 7118 100.0U UFCVM

b
15KV X1200 7119 10.0U UFCVM

FIGURE 19. SCANNING ELECTRON MICROSCOPY OF CORROSION CASTS. a. The branch point of a cilioretinal arteriole with an annular constriction may represent a sphincter mechanism for regulation of retinal blood flow. (1,800 X.) b. Distended vessels forming oval structures (arrow) are probably a result of excessive perfusion pressure. Undigested tissue is also present. (72 X.)

19a
15KV X1800
120
10.0U UFCVM

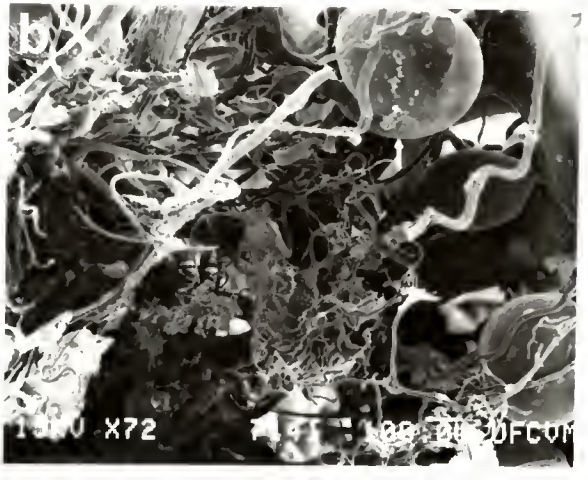
b
X72

FIGURE 20. SCANNING ELECTRON MICROSCOPY OF CORROSION CASTS. a. One oval structure is drained by a vessel with oval mural impressions suggesting it is of venous origin (arrow). (200 X.) b. A distended sphere of casting material in a vascular structure is present. (160 X.)

20a
15KV X200 7142 100

b
15KV 7143

FIGURE 21. SCANNING ELECTRON MICROSCOPY OF CORROSION CASTS. a. A SPCA "pillar" branches into cilioretinal and larger diameter choroidal arteries. Filling defects are seen in the proximal end of the SPCA (arrow). (94 X.) b. Filling defects are also present in this SPCA (arrow). (160 X.)

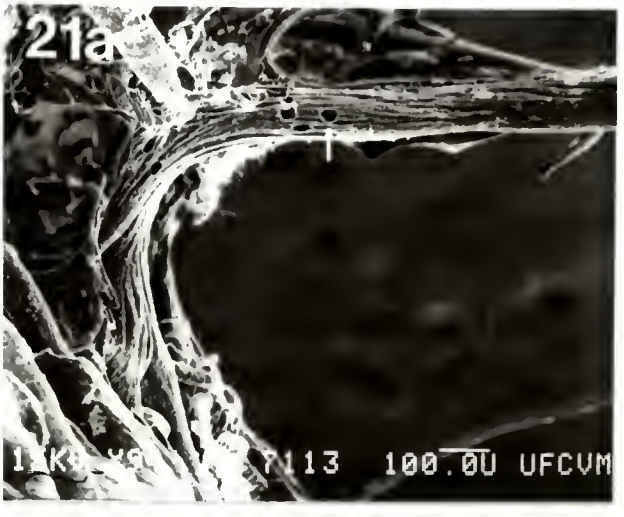
21a
7113 100.0U UFCVM

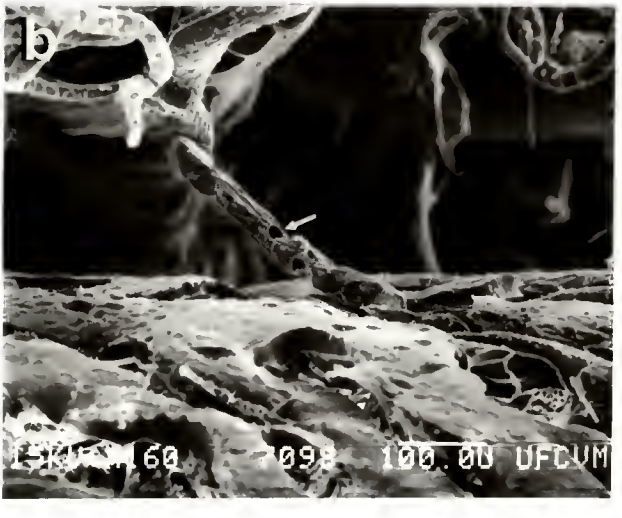
b
100.0U UFCVM

FIGURE 22. SCANNING ELECTRON MICROSCOPY OF CORROSION CASTS. a. Casting material coats the longitudinal striations of this SPCA. A filling defect is also present (star). (540 X.) b. Casting material leaks through the interendothelial cell junctions in a few vessels to cause this ribbon appearance (arrows). (1,800 X.)

22a
15KV X540
10.0U UFCVM

b
15KV X1800 7122
UFCVM

FIGURE 23. COMPOSITE DRAWING OF FIGURES 1, 3, 5, 9-11. The arteries to the globe supply a radial series of pillar-like SPCA which provide blood to the retina, via cilioretinal arteries, and to the choroid. Most choroidal venous drainage is anterior as the choroidal veins are blind ended at the scleral canal.

Fig. 23

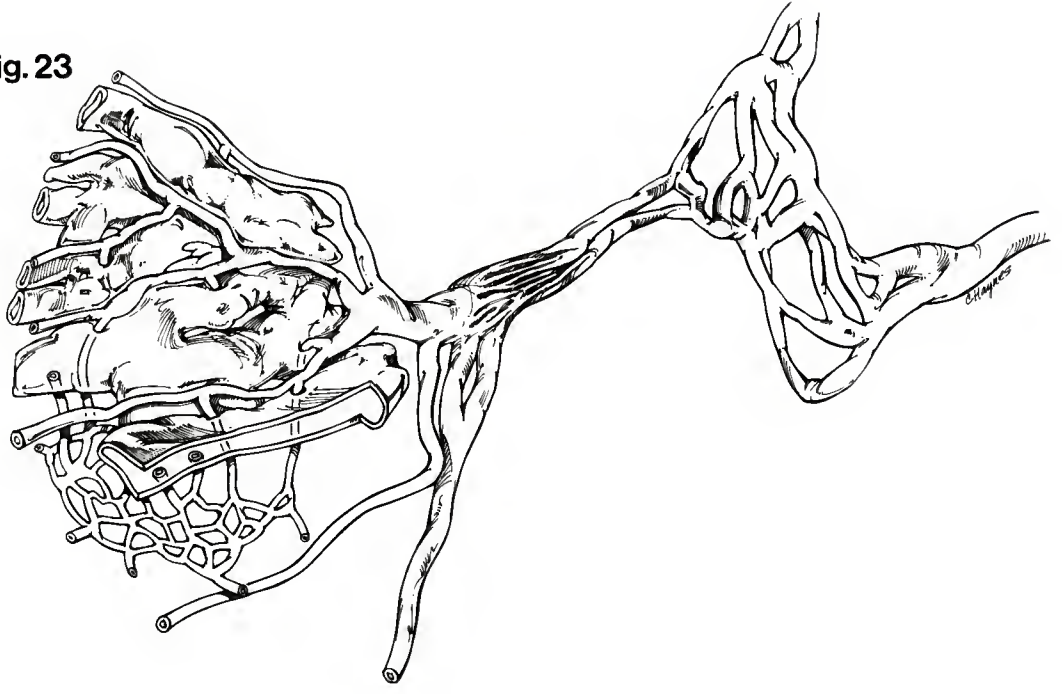

FIGURE 24. COMPOSITE DRAWING OF FIGURES 1, 3-5. This illustration of the posterior microcirculation shows the widely anastomotic set of vessels surrounding the orbital optic nerve.

Fig. 24

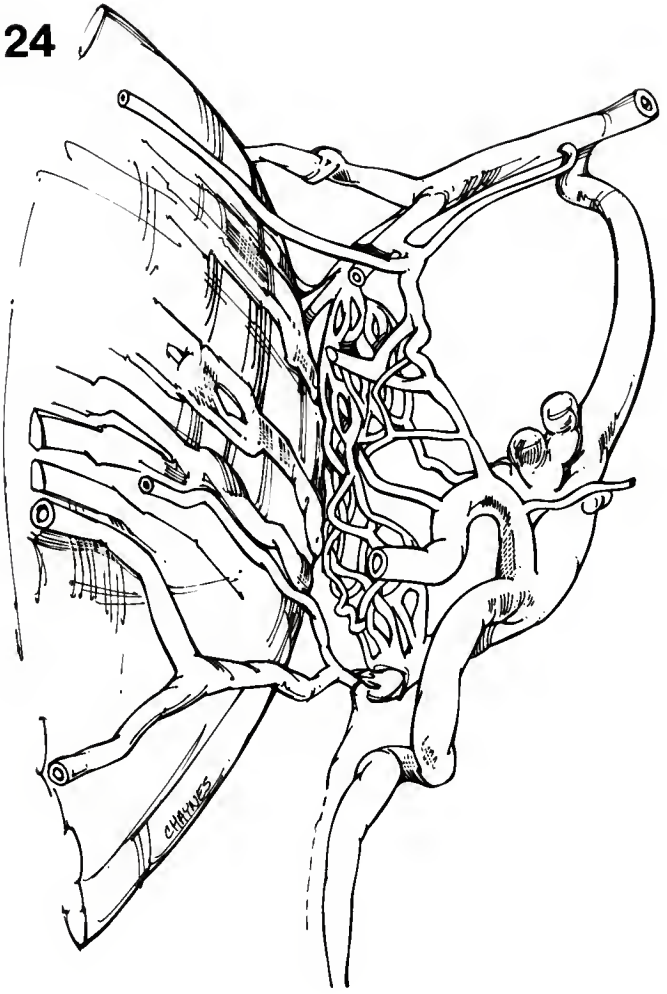

FIGURE 25. COMPOSITE DRAWING OF FIGURES 4-6. Large saccular structures are noted posterior to the SPCA in a few dogs. They appear to be more vein-like than arterial, but the vascular origin was not determined.

Fig. 25

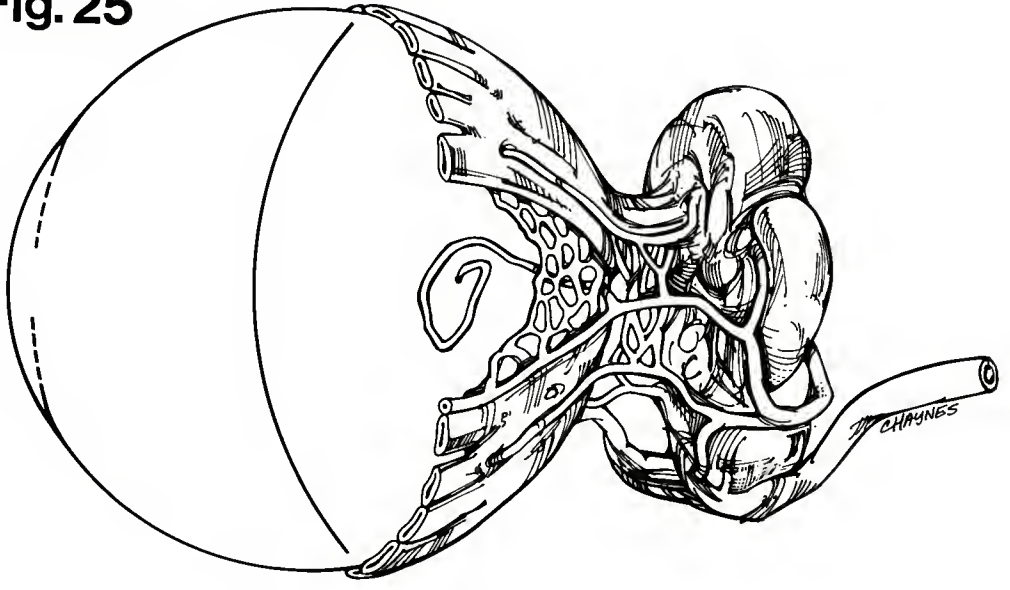

FIGURE 26. COMPOSITE DRAWING OF FIGURES 7, 9, 15, 16. Cilioretinal arteries are depicted entering the globe at the scleral canal. Cilioretinal veins are present and incompletely filled, but their exact site of posterior drainage was not determined.

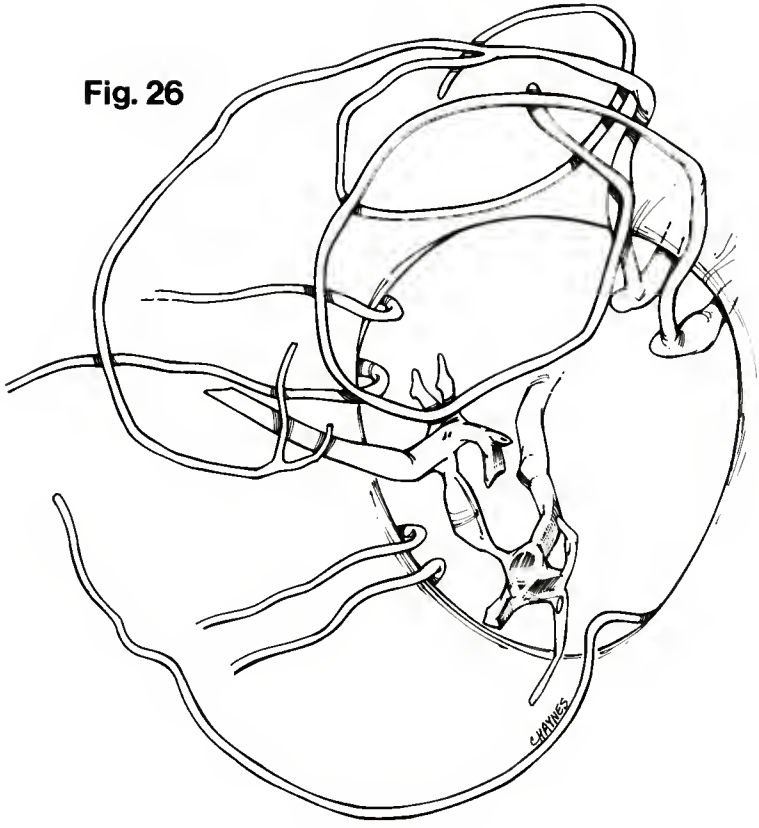
Fig. 26
C.HAINES

DISCUSSION

Axoplasmic transport in the optic nerve axons of Beagles with primary open angle glaucoma, as studied with autoradiography was impaired at the scleral lamina cribrosa.[21,22] Ultrastructural changes included optic nerve demyelination early in the disease, glial cell hypertrophy and hyperplasia, and the accumulation of intracellular organelles in swollen (dilated) axons at the scleral lamina cribrosa. Glial tissue became more prominent as the disease progressed. These changes were similar to those previously demonstrated in the human, rat, nonhuman primate, and cat.[11,19-22,24]

This study demonstrated a significant change in the supporting architecture of the optic nerve that increased in degree as the disease progressed, thus having indicated a partial effect at early stages of the disease when the IOP was only slightly elevated. Pathologic morphologic changes of the lamina cribrosa accompanied early to moderately affected Beagle dogs with primary open angle glaucoma. These changes were present before the detection of overt ophthalmoscopic changes in the optic nerve head. One of the most interesting aspects of primary open angle glaucoma in the dog is the relatively long period of latency, a period of time when biologically significant changes are occurring in the optic nerve tissue, but are too minimal to be detected by present clinical means.

It is interesting to speculate on the changes of the lamina cribrosa that result from the elevated IOP to cause optic nerve atrophy and blindness. An increased IOP would result in an increase in the difference between the IOP and the retrobulbar tissue pressure.[9] Oepending on the magnitude of the pressure elevation, and the relative resistance to deformation inherent in the lamina cribrosa and the intravascular pressure of the laminar capillaries, the laminar beams bridging the scleral canal are displaced posteriorly. While the exact time of the posterior bowing of the lamina could not be elicited in this study, it clearly occurs in the early to moderate phase of this disorder, and eventually results in optic nerve cupping and atrophy.

As the IOP increases, the circumferential force or scleral wall tension inherent in any sphere would also become elevated. It seems reasonable to expect that the lamina cribrosa would also be affected by the increased wall tension. Less dense areas of the laminar supporting tissue would initially become distorted in shape and could lead to a change in the shape of the pores and to a misalignment of successive laminar sheets. The increased wall tension is thus transmitted to the nerve bundles.[9]

A mechanical deformation of the lamina occurring early in the disease process would strengthen the argument that this deformation was responsible for the initial or inciting cause of glaucomatous optic nerve damage. It should be remembered that the capillaries which supply the laminar nerve bundles are also contained in the laminar connective tissue sheets and could also be compromised by the laminar mechanical distortion, resulting in concomitant

perfusion-deficit ischemia to the nerve bundles. This study is unable to resolve which component is the primary instigator of glaucomatous optic nerve damage, but suggests that both mechanisms may be affecting the optic nerve axons.

The trypsin digest technique dramatically revealed the supporting architecture of the optic nerve region. A detergent digestion of an unfixed specimen did not appear to digest and remove enough neural and glial tissue to analyze the specimen adequately, although one researcher had excellent results using detergent digests of autolyzed human necropsy specimens.[9] The retrolaminar myelinated nerve fibers were more resistant to the trypsin digestion. Eyes in early stages of glaucoma were more difficult to digest, possibly due to the presence of more healthy myelinated nerve fibers.

The digested tissue from the experimental ocular hypertensive dog resembled that from a moderately affected Beagle dog in terms of the amount of laminar distortion present. This is interesting as the dog was normal. It is known that optic nerve cupping is reversible in some human patients, but permanent cellular changes were indicated in this experiment. The elevated IOP in humans will cause transient movement in the lamina cribrosa due to inherent elasticity.[63] Elastin was present in the canine lamina cribrosa, so the potential for reversible movement exists. Evidently, even acute elevations in IOP in normal dogs can cause significant cellular alterations of the lamina cribrosa.

The most striking feature of the optic nerve laminar capillaries in Beagle dogs with primary open angle glaucoma was the presence of the electron-dense inclusions within the endothelial cells. These

inclusions were most often spherical. Some were tubular or cylindrical and in most instances had no visible substructure. In a few inclusions a tubular infrastructure could be detected. The cylindrical dense bodies with a tubular infrastructure are probably Weibel-Palade bodies, a cytoplasmic organelle specific to vascular endothelial cells.[64] Cylindrical electron-dense inclusions without a tubular infrastructure may represent degenerated forms of Weibel-Palade bodies, degenerate mitochondria, bundles of microfilaments, cytoplasmic granules or other dense bodies.[64]

Weibel-Palade bodies are rod-shaped cylindrical cytoplasmic organelles specific to endothelial cells. They are 0.1 to 0.4 microns in width, up to 2.5 microns long,[65-67] and are bounded by a limiting membrane. A tubular substructure can usually be detected. Immature forms have been associated with the Golgi apparatus which may be the site of origin.[66,67] Weibel-Palade bodies are reported in vascular endothelia of toads,[68,69] and ocular vascular endothelia of rabbits, nonhuman primates and man.[65-67] The tubular substructures are believed to consist of parallel aggregates of von Willebrand's protein and may be a storage and processing organelle for this protein.[64] Their numbers are elevated in brain neoplasms,[64] Behcet's disease,[66] thrombosed regions,[65] glaucoma,[70] and are decreased in human iris vessels in the presence of senile cataract.[70] They represent normal components of ocular vascular endothelia which appear early in the development of the eye, and increase in number when circulatory disturbances occur.[64,66,67]

The membrane bound, rod-shaped, electron-dense inclusions found in normal dogs and in the Beagle dogs with primary open angle

glaucoma are similar in size, shape and appearance to previously described Weibel-Palade bodies. The tubular substructures were not always detected in our specimens or those of other authors.[64] There were substantially increased numbers of the electron-dense inclusions in the laminar capillaries of affected Beagles prior to expression of the disease. As Weibel-Palade bodies are known to be associated with diseases which have circulatory disturbances, this study demonstrated an ultrastructural difference between the laminar capillary endothelial cells of normal and affected Beagle dogs that could be associated with a functional vascular disorder.[64,67,70,89] Although these inclusions in the Beagles with POAG have been speculatively associated with some function, such as anticoagulation[65] or intraocular pressure regulation,[70] it is difficult to make functional interpretations solely on the morphologic evidence in this study. I am thus unable to provide a simple vascular explanation for the obstruction of axoplasmic flow that occurs in the optic nerve of Beagles with primary open angle glaucoma.[22]

Mechanical and vascular theories have been proposed as the cause of axoplasmic flow obstruction in optic nerves and subsequent optic nerve atrophy of glaucomatous eyes.[3-8,10,13,15-23,71,72] Compressive distortion of the optic nerve axon bundles as they pass through the openings of the scleral lamina cribrosa has recently been demonstrated in man.[9] This mechanical distortion would also cause secondary ischemic changes due to disturbance of the microcirculation in the optic nerve capillaries contained within the scleral lamina cribrosa's trabecular beams.[8]

Several mechanisms have been proposed to cause ischemic optic nerve damage in glaucoma from vascular insufficiency.[72] Gafner and Goldmann proposed that shunting of blood from the optic nerve head to other areas would occur if the arterial pressure in the vessels supplying the optic nerve was normally relatively low. An increase in intraocular pressure that affected retinal blood flow a slight amount might significantly reduce blood flow in the optic nerve.[73] Hayreh proposed that glaucomatous optic nerve degeneration was associated with choroidal artery compression that disturbed the centripetal optic nerve microcirculation from the pial vessels.[74] Neither of these theories was supported by a radiolabeled microsphere study of the blood flow to the optic nerve region.[72] Alm and Bill suggested that autoregulation of the optic nerve microcirculation might be defective in human glaucomatous eyes.[25] Recent evidence indicates that autoregulation of retinal arterioles is defective in humans with primary open angle glaucoma.[75] The macular retinal blood flow may be compromised during periods of increased intraocular pressure. These authors proposed that a similar regulatory abnormality may be present in the human optic nerve microcirculation, although this was not supported by other experiments which show efficient autoregulatory capabilities in the nonhuman primate prelaminar optic nerve.[72] The study of the optic nerve of young monkeys with acute experimental ocular hypertension to determine the effects of chronically elevated IOP on the human optic nerve may therefore differ from the effects seen in humans or Beagle dogs with the chronic IOP elevation of POAG. The autoregulatory ability of the optic nerve of the experimental monkey is probably normal and could yield conflicting functional data.

Autoregulation of blood flow is defined as an intrinsic homeostatic mechanism that maintains constant blood flow to an organ despite changes in local arterial perfusion pressure.[76,77] The perfusion pressure of the eye is the mean arterial blood pressure minus the intraocular pressure. Autoregulation has been demonstrated in the brain, kidney, intestine, myocardium and liver.[72]

Iris and ciliary body blood flow is autoregulated in cats and monkeys.[25] No autoregulatory capability is present in the choroid.[25] Efficient autoregulatory function is found in the retina of monkeys, cats, pigs, rabbits and man.[25,77,78] Autoregulation of the prelaminar optic nerve occurs over a wide range of intraocular pressures in monkeys,[72] and occurs from 110-120 mmHg in the canine.[79]

Intrinsic microvascular control systems allow the microcirculation to respond to the specific needs of the tissue it subserves. Autoregulation is the local resistance response that tends to stabilize flow in spite of altered input pressure.[80] Obstruction of arterial inflow or increased activity of a tissue causes intrinsic vasodilatation.

Metabolic and myogenic theories are proposed to explain the process of vascular autoregulation.[80] The metabolic hypothesis says that a feedback system exists between cellular metabolism and the tone of the microvessels exerting control over blood perfusion and distribution. Tissue oxygenation or other metabolites modulate the vascular tone. Abnormal glycosaminoglycans (GAG) in the lamina cribrosa could alter normal autoregulatory responses. The myogenic theory of autoregulation relies on inherent properties of vascular smooth muscle.[80]

The myogenic hypothesis is believed to explain the prominent autoregulatory capabilities of the anterior uveal tissues.[25,76] No smooth muscle is present in the optic nerve capillaries of the dog, but autoregulatory capability may not require an elaborate ultrastructural device in order for local biochemical alterations to influence the endothelial cells and pericytes of the microvasculature.

It is not possible to decide from this study whether capillaries can or cannot contract. The pericyte may be contractile as it is believed to be a precursor to smooth muscle cells, but if such contraction were to occur it would be indistinguishable from ameboid movements,[81] as this cell type lacks any definable myocontractile apparatus. Microfilaments were seen in the endothelial cells of dogs, but these were probably adaptations for strength from shearing forces rather than myofilaments. It is possible that endothelial cells could demonstrate some degree of ameboid type contractility or that endothelial cell swelling in response to a metabolic biochemical stimulus could result in the endothelial nucleus passively blocking the vascular lumen.[81,82] It is not considered likely, however, that capillary endothelial cells can actively contract upon stimulation.[82] Regulation of flow through the optic nerve microcirculation probably occurs at the level of the arteries or arterioles that supply this region. Choroidal arteries may be too far away to be influenced by metabolites accumulating in the optic nerve tissues,[72,73] but cilioretinal or SPCA could be involved.

It is difficult to determine the microvascular supply to the optic nerve. Anatomical data is conflicting, contradictory and species specific.[28,33,36,39,40,42,53,83] In normal eyes, only

ophthalmoscopy allows observation of the largest retinal and choroidal vessels. Neither fluorescein angiography nor infrared indocyanin green angiography permit accurate study of the microanatomy of the optic nerve circulation as the area is small and the blood flow rapid. The intrascleral and intrachoroidal portion of the ciliary artery circulation cannot be visualized using any of these techniques so the accurate distribution of each artery is impossible to determine in vivo.[53]

Scanning electron microscopy of methylmethacrylate corrosion casts provided an excellent three dimensional representation of the optic nerve angioarchitecture.[34] The modified Batson's compound was of low enough viscosity to penetrate to the capillary level and stable enough to provide extremely detailed information of vascular connections and distribution under heavy electron bombardment.[38] Information provided from vascular corrosion casts compared favorably with histological sections, in vivo photographs, and whole mounts of vessels.[44]

Interpretation of data obtained from vascular casts must be tempered by consideration of artefactitious luminal dilatation due to nonphysiologic viscosity and elevated filling pressure, incomplete filling of vessels manifested by bubble formation or disruption of the endothelial cell nuclear impressions, incomplete digestion of tissue resulting in opaque membranes, and extravasation of plastic between endothelial cells causing beads, mounds and smooth surfaced globules.[49,50] Underperfusion and questionable measurements of lumenal diameter limit the physiologic deductions about vessel caliber and flow dynamics that can be made from the study of castings.

They do not preclude, however, statements regarding the existence of vascular channels, their spatial relationships and their interconnections.[33,45,49,50,84,85]

The injection of the Batson's compound using gentle hand pressure provided satisfactory results in most of the canine eyes as assessed by the presence of endothelial cell nuclear impressions of the small and large diameter-sized vessels. Nuclear endothelial cell mural impressions indicate adequate filling of casting material.[51] Plastic strip artefacts and the appearance of isolated spheres of plastic compound indicated some vessels were overperfused while shrinkage, vessel surface distortion, and pitting in other casts indicated slight underfilling.[50] The short posterior ciliary veins (SPCV) and retinal capillaries were most affected by underfilling. Incomplete tissue digestion was rare but noted in a few instances. The most pronounced artefact in this series of canine eyes was a generalized saccular enlargement in large diameter-sized vessels posterior to the laminar region. This is most likely associated with elevated perfusion pressure or overfilling of cast material and appeared confined to venous structures, but the detail necessary to determine the vessel type was obscured.

The vascularity of the human optic nerve was first studied by Zinn and Haller in the 1750's.[86] They described a radial anastomotic network of intrascleral branches from short posterior ciliary arteries (the closed arterial circle of Zinn and Haller) forming anastomoses with capillaries of the anterior optic nerve and branches of the central retinal artery.

Hayreh[83] suggested that the prelaminar optic nerve of primates was supplied by centripetal branches of the choroidal vessels with no contribution by the central retinal artery. The lamina cribrosa was in his view entirely supplied by centripetal branches of short posterior ciliary arteries. The intrascleral circle of Zinn and Haller was a rare finding. The retrolaminar optic nerve in Hayreh's opinion also derived its blood supply from the posterior ciliary arteries. Current opinion[28,33,34] is that the human and nonhuman primate prelaminar optic nerve is supplied by centripetal branches of short posterior ciliary vessels that have coursed anteriorly in the choroid, with the lamina cribrosa supplied by transverse arterioles from scleral short posterior ciliary arteries and pial vessels.[28,33] A dense capillary plexus surrounds the anterior optic nerve.[45] Longitudinal anastomoses of capillaries of the retina and optic nerve occur.[33] There is no communication between the optic disc capillary system and the choriocapillaris.[28,33,34] The role of the central retinal artery in humans and nonhuman primates is controversial, but is probably of little importance in supplying the laminar optic nerve.[28,41]

The vasculature of the domestic feline eye has been studied by casting methods[37,38] and dissection.[39] Long posterior ciliary arteries send branches to the retrolaminar optic nerve to form a ring-like dense vascular annulus. From this annular plexus emerge branches for the retina and choroid which pierce the sclera adjacent to the optic nerve.

There are neither individual short posterior ciliary arteries surrounding the entrance of the optic nerve, a circle of Zinn-Haller,

nor a central retinal artery in the feline as is seen in humans and nonhuman primates.[37] Posterior to the lamina cribrosa, the optic nerve received nutrition from longitudinal pial branches.[87] One author described cilioretinal arteries surrounding the optic nerve.[38] The blood supply to the lamina cribrosa of the feline was not specifically described, but a rich capillary plexus in that region could be seen in a scanning electron micrograph.[38] The venous drainage to the feline eye was from the vortex veins, intrascleral plexus and a plexus of vessels surrounding the optic nerve. Peripapillary veins were internal to the arteries.[37] The terminology of the vessels was obviously confusing to the two authors.[37,38]

Duke-Elder[40] and Prince[39] described the vasculature of the canine optic nerve as without a central retinal artery, and suggested the posterior ciliary vessels and cilioretinal arteries as the predominant vessels to the optic nerve and retina. The ciliary arteries of the canine were described as having "subendothelial cushions", which hypothetically functioned to divert blood from the choroidal to the retinal circulation.[40] The circulation to the lamina cribrosa specifically was not described, although some authors described a Circle of Zinn-Haller for the dog.[86]

This report is the first to attempt to determine the complete microcirculatory pattern to the canine optic nerve. Several features appear to be unique to the dog. The short posterior ciliary arteries form a set of six to ten pillars surrounding the laminar optic nerve. These vessels had deep longitudinal striations that may be either vascular smooth muscle which had undergone vasospasm as a result of

the introduction of casting material, or may be linear patterns of endothelial and pericyte cytoplasm. Light microscopy of sections through this area revealed prominent smooth muscle in the short posterior ciliary arteries. The short posterior ciliary arteries branched to form prominent choroidal arteries and retinal arterioles. The retinal arterioles had annular constrictions at vessel branch points that may be involved in the regulating of blood to the retinal and laminar circulations. The derivation of the laminar capillaries from the short posterior ciliary arteries and longitudinal pial vessels, and their anastomosis with the retinal capillaries was similar to the primate pattern. The canine posterior ciliary arteries supplied the capillaries to the retina and optic nerve, and to the noncommunicating choroidal capillary system. The lack of a central retinal artery in the dog was similar to the cat. The laminar capillary plexus appeared more dense in scanning micrographs of the nonhuman primate and cat, than in these canine specimens.[38,45] The saccular vein-like structures posterior to the short posterior ciliary arteries were unique to the dog, but similar in location to the posterior veins of the rat.[36] Venous drainage appeared to move anteriorly toward the vortex system in the dog.

The predominance of the ciliary arteries in the circulation to the optic nerve of the dog may provide an anatomical mechanism for the homeostatic maintenance of optic disc perfusion due to ciliary artery autoregulation during episodes of elevated IOP. The ciliary arteries provide nutrition to both the choroidal and retina-optic nerve systems. The cilioretinal vessels could also play a role in the blood supply to the lamina cribrosa due to their proximity to the

region. Experimental microsphere studies in nonhuman primates indicated that blood flow in the retina and anterior optic nerve was not significantly affected by a wide range of intraocular pressures indicating autoregulatory capacity of the supplying blood source.[25] These vessels may also be resistant to compression and collapse. The oxygen supply to the feline retina was also adequate over a wide range of intraocular pressures.[25] It may be that a similar autoregulatory capacity is present in the circulation to the canine optic nerve.

The ciliary arteries in the dog and the cat are fed primarily by branches of the external ophthalmic artery, whereas the ciliary arteries of humans and nonhuman primates receive their blood predominantly from the internal ophthalmic artery.[39,40] The external ophthalmic artery is a branch of the external carotid artery, while the internal ophthalmic artery is a branch of the circle of Willis. The arterial supply to the dog is therefore of extracranial origin, while primates have an intracranial supply. The microvasculature of the central nervous system possesses dramatic autoregulatory capacity, with variable regulatory capability in other tissues of the body.[25] The significance of this to the dog is not known, but may have functional implications to optic nerve regulatory capability.

Nonhuman primates with experimentally induced ocular hypertension failed to fill the capillaries of the laminar circulation with casting material to the same degree as normal animals in one study.[41] Vascular casts of eyes from nonhuman primates with experimentally induced glaucoma in another study revealed retinal capillary dilatation, "polymorphous caving" of deep

retinal capillaries suggesting endothelial cell damage, and absence of a dense prelaminar capillary plexus in the glaucomatous eye as compared to the control eye.[88]

Vascular casting has also been used previously to document arteriovenous crossing defects in a hypertensive man, microaneurysms and localized areas of nonperfusion of the retinal capillaries in a diabetic woman, and choroidal neovascularization in an infant with retinopathy of prematurity.[89,90] Vascular casts of retinal and subretinal neovascularization in primates[48] and rabbits,[51] and corneal neovascularization in rats[49] have been examined.

This study demonstrated that there is no appreciable difference in casting morphology of the optic nerve vasculature between normal dogs and beagles with glaucoma, but did not address the function or flow capacity of these vessels. The ability to fill a vessel with casting material is no indication of its physiological capacity in vivo, but only provides information for enthusiastic speculation. Some capillaries examined in experiment two had collapsed lumens in spite of the employed perfusion fixation technique. It is possible that some regions of the optic nerve were underperfused.

SUMMARY

Definitive answers to the three hypotheses were obtained. No three dimensional differences in the angioarchitecture of the optic nerves of normal and glaucomatous Beagle dogs were detected by scanning electron microscopy of corrosion casts. Lesions had been detected in casts of glaucomatous monkeys and humans with various ocular abnormalities in other studies.[41,88-90]

The microcirculation to the lamina cribrosal region in the dog was derived from the short posterior ciliary arteries, cilioretinal arteries, longitudinal pial vessels, and anastomoses with retinal capillaries. It appears from studies in other species[25] that the laminar optic nerve microcirculation has autoregulatory capability in the face of increased intraocular pressure or reduced perfusion pressure.

Optic nerve capillary endothelial cells of glaucomatous Beagle dogs are ultrastructurally abnormal prior to detectable elevations in intraocular pressure. Functional alterations in the microcirculation to the optic nerve of glaucomatous Beagle dogs may therefore have a structural basis. The abundant electron-dense inclusions noted are probably Weibel-Palade bodies which are known to increase in number when circulatory disturbances are present.[66] It is highly speculative, but still suggestive, that deficits in endothelial cell function resulting in local tissue ischemia and capillary leakage are

present early in glaucoma in the Beagle and may contribute to axonal demyelination, reduction in axoplasmic flow, and glial cellular changes. Vascular insufficiency may become most important in the pathologic process when the perfusion pressures are severely reduced by extreme rises in intraocular pressure.

It is difficult to make definitive statements concerning the relationship of ultrastructural morphology and function. The electron-dense inclusions or Weibel-Palade bodies may be a response to a microcirculatory problem or may actually be causing a microcirculatory abnormality. The inclusions noted may physically impair the cell's normal function, or liberate some metabolite to aid or cause any tissue circulatory disturbances. Physically altered sclerotic arteries and arterioles in humans are believed to have reduced autoregulatory capabilities.[72] Compromise of the microcirculation could also be associated with the mechanical compression of the capillaries in the collagenous laminar trabecular beams, which result in the formation of more Weibel-Palade bodies, and not be a primary event.

This study is not able to define blood flow abnormalities in this tissue. The presence of red blood cells in some capillaries may suggest that the capillaries were perfused, although they could still be functionally abnormal. Normal retinal blood flow in spite of capillary perfusion abnormalities and defective autoregulation is known to occur in other ocular diseases, such as diabetes.[90]

It was confirmed in the examination of trypsin digests of the optic nerve lamina cribrosa that posterior laminar displacement with misalignment of the laminar fenestrations was progressive and

occurred prior to overt ophthalmoscopic changes. This is similar to humans with glaucoma in that significant pathology occurs to the optic nerve axons at the lamina cribrosa prior to the detection of visual field loss.[11] Compression of the anterior, middle and posterior layers of the lamina cribrosa was most prominent in Beagles at the advanced stage of the disease.

Support for both the mechanical and vascular theories of glaucomatous optic nerve damage was found in the affected Beagle dog. The mechanical compression of axon bundles would appear to have a more visible and dramatic effect in the affected Beagle, but subtle disturbances in the microcirculation, if they exist, may be associated with reduced ability to respond to elevations in intraocular pressure. Compression of capillaries in the trabecular beams would also cause indirect secondary ischemic damage to axon bundles. Circulatory disturbances of the optic nerve microcirculation, as evidenced by the tubular electron-dense inclusions, may be present prior to the pressure induced distortion of the laminar cribrosa. The optic nerve of affected Beagle dogs may be less able to adjust to the elevations in intraocular pressure (and reduced perfusion pressure) than a normal animal. Retinal autoregulatory capabilities are known to be deficient in humans with glaucoma.[75,77] It is interesting to speculate that these ultrastructural features in affected Beagle dogs are also indicative of some functional disorder of the optic nerve capillaries. Functional studies to determine normal canine optic nerve flow patterns are warranted to find out if circulatory disturbances are indeed present in the Beagle dog with POAG.

One of the original objectives of this study was to explain why dogs that develop glaucoma tolerate the elevated pressure for a time, and then rapidly develop severe optic nerve cupping and atrophy in spite of aggressive therapy. Elastin fibers were detected in the canine lamina cribrosa and thus may allow for some stretching or "give" to occur. The nerve fibers are myelinated in the canine anterior to the optic disc and could be partially protected by their lower metabolic activity[25] in conditions of vascular compromise, although demyelination in the prelaminar optic nerve is one of the earliest ultrastructural changes seen in affected Beagles.[22] The most likely cause for the delay in cupping and optic nerve atrophy appears to be the existence of a large number of nerve fibers. The nerve fibers are continually damaged as the intraocular pressure remains elevated. In some species, specific regions and specific sized fibers of the optic nerve are affected first, but eventually all fibers become susceptible.[11] No regional differences in the canine lamina cribrosa were detected. Damage to nerve fibers may make other fibers more susceptible to damage.[22] Eventually enough nerve fibers are injured so that visual field defects occur. Over half the nerve fibers are destroyed prior to the development of visual field deficits in humans.[11] Humans are able to retain a central visual acuity of 20/20 to 20/30 with 80% of the nerve fibers destroyed.[11,91] No such data exists for the dog, but a substantial amount of damage must be present for the dog to develop optic nerve cupping and atrophy, and blindness.

Individual variability between optic nerves of human patients exists to allow variable tolerance to the elevated intraocular

pressure.[11] There are undoubtedly also species differences. This author believes that certain breeds of dogs with primary glaucoma also appear more tolerant of elevated intraocular pressures than other breeds.

A common factor causing glaucoma and its optic nerve damage has been sought for in the anterior and posterior segments of the eye. A combined anterior and posterior connective tissue weakness is a possibility.[25] The sclera extends anteriorly as the corneoscleral trabecular meshwork (CSTM) and posteriorly as the inner layers of the lamina cribrosa. Weakness in the CSTM could result in abnormal filtering of aqueous humor with weakness in the lamina cribrosa making it more pressure sensitive. Greater weakness in the CSTM could result in glaucoma with very high intraocular pressures, while greater weakness in the anterior lamina cribrosa could result in severe optic nerve damage at near normal intraocular pressures, i.e. low tension glaucoma.[25,92] Examination of collagen structure and organization is warranted in these ocular regions. Local and systemic vascular disorders might also play an important role in low tension glaucoma.[25,92] Optic nerve hemorrhage from capillary stretching and mechanical compression could cause local vasoconstriction in the optic nerve as occurs in the brain following hemorrhage.[25]

Accumulation of abnormal glycosaminoglycans (GAG), in the corneoscleral trabecular meshwork (CSTM) and lamina cribrosa could alter normal function of these structures. A hyaluronidase resistant GAG is known to be present in the CSTM of the glaucomatous Beagle dog.[93] The effect of such a GAG in the canine lamina cribrosa is not

known, but could interfere with oxygen or metabolite diffusion in a manner that will negate or alter the normal autoregulatory feedback system.

Future studies in the normal and glaucomatous Beagle dog should include estimation of optic nerve blood flow using radiolabeled microspheres or preferably the ^{14}C-deoxyglucose method of Sokoloff.[25] Autoregulation of ocular blood flow could be evaluated by measuring visual evoked potentials during periods of elevated IOP.[94] Biochemical evaluation of the lamina cribrosa for changes or accumulation of GAG could provide information as to the presence of a connective tissue weakness in the lamina cribrosa and CSTM.

BIBLIOGRAPHY

1. Gelatt, KN: Inherited Primary Glaucoma in the Beagle. Am. Soc. Vet. Ophthalmol., Las Vegas, NV, pp 116-119, 1982.

2. Gelatt, KN, Gum, GG, Gwin, RM, Bromberg, NM, Meredith, RE, Samuelson, DA: Inherited Primary Open Angle Glaucoma in the Beagle. Am. J. Path. 102(2):292-295, 1981.

3. Quigley, HA, Addicks, EM, Green WR: Optic Nerve Damage in Human Glaucoma. III. Quantitative Correlation of Nerve Fiber Loss and Visual Field Defect in Glaucoma, Ischemic Neuropathy, Papilledema, and Toxic Neuropathy. Arch. Ophthalmol. 10:135-146, 1982.

4. Emery, JM, Landis, D, Paton, D, Boniuk, M, Craig, JM: The Lamina Cribrosa in Normal and Glaucomatous Human Eyes. Trans. Am. Acad. Ophthalmol. Otol. 78:OP290-OP297, 1974.

5. Quigley, HA, Hohman, RM, Addicks, EM, Massof, RW, Green, WR: Morphologic Changes in the Lamina Cribrosa Correlated with Neural Loss in Open-Angle Glaucoma. Am. J. Ophthalmol. 95(5):673-691, 1983.

6. Anderson, DR: Ultrastructure of Human and Monkey Lamina Cribrosa and Optic Nerve Head. Arch. Ophthalmol. 92:800-814, 1969.

7. Radius, RL, Gonzales, M: Anatomy of the Lamina Cribrosa in Human Eyes. Arch. Ophthalmol. 99:2159-2162, 1981.

8. Minckler, D, Spaeth, G: Optic Nerve Damage in Glaucoma. Surv. Ophthalmol. 26(3):128-148, 1981.

9. Quigley, H, Addicks, E: Regional Differences in the Structure of the Lamina Cribrosa and Their Relation to Glaucomatous Optic Nerve Damage. Arch. Ophthalmol. 99:137-143, 1981.

10. Radius, RL: Regional Specificity in Anatomy at the Lamina Cribrosa. Arch. Ophthalmol. 99:478-480, 1981.

11. Quigley, HA, Addicks, EM, Green, WR, Maumenee, AE: Optic Nerve Damage in Human Glaucoma. II. The Site of Injury and Susceptibility to Damage. Arch. Ophthalmol. 99:635-649, 1981.

12. Rohen, JW: Why is Intraocular Pressure Elevated in Chronic Simple Glaucoma? Ophthalmol. 90(7):758-765, 1983.

13. Quigley, HA, Flower, RW, Addicks, EM, McLeod, OS: The Mechanism of Optic Nerve Damage in Experimental Acute Intraocular Pressure Elevation. Invest. Ophthalmol. 19(5):505-517, 1980.

14. Quigley, HA, Hohman, RM, Addicks, EM: Quantitative Study of Optic Nerve Head Capillaries in Experimental Optic Disk Pallor. Am. J. Ophthalmol. 93:689-699, 1982.

15. Zimmerman, LE, de Venecia, G, Hamasake, OI: Pathology of the Optic Nerve in Experimental Acute Glaucoma. Invest. Ophthalmol. 6(2):109-125, 1967.

16. Radius, RL, Anderson, OR: Rapid Axonal Transport in Primate Optic Nerve. Arch. Ophthalmol. 99:650-654, 1981.

17. Maumenee, AE: Causes of Optic Nerve Oamage in Glaucoma. Ophthalmol. 90(7):741-752, 1983.

18. Anderson, DR: What Happens to the Optic Disc and Retina in Glaucoma? Ophthalmol. 90(7):766-770, 1983.

19. Radius, RL, Bade, B: The Anatomy at the Lamina Cribrosa in the Normal Cat Eye. Arch. Ophthalmol. 100:1658-1660, 1982.

20. Radius, RL, Bade, B: Axonal Transport Interruption and Anatomy at the Lamina Cribrosa. Arch. Ophthalmol. 100:1661-1664, 1982.

21. Williams, LW, Gelatt, KN, Gum, GG, Samuelson, DA, Meredith, RE: Orthograde Rapid Axoplasmic Transport and Ultrastructural Changes of the Optic Nerve. Part I. Normotensive and Acute Ocular Hypertensive Beagles. Glaucoma 5(3):117-128, 1983.

22. Samuelson, OA, Williams, LW, Gelatt, KN, Gum, GG, Meredith, RE: Orthograde Rapid Axoplasmic Transport and Ultrastructural Changes of the Optic Nerve. Part II. Beagles with Primary Open Angle Glaucoma. Glaucoma 5(4):174-184, 1983.

23. Hayreh, SH: Anatomy and Physiology of the Optic Nerve Head. Trans. Am. Acad. Ophthalmol. Otol. 78:OP240-OP252, 1974.

24. Johansson, J: Inhibition of Retrograde Axoplasmic Transport in Rat Optic Nerve by Increased IOP In Vitro. Invest. Ophthalmol. 24(12):1552-155B, 1983.

25. Bill, A: Some Aspects of the Ocular Circulation. Invest. Ophthalmol. 26(4):410-424, 1985.

26. Gelatt, KN, Peiffer, RL, Gwin, RM, Gum, GG, Williams, LW: Clinical Manifestations of Inherited Glaucoma in the Beagle. Invest. Ophthalmol. 16(12):1135-1142, 1977.

27. Gelatt, KN: Animal Models for Glaucoma. Invest. Ophthalmol. 16(7):592-595, 1977.

28. Anderson, DR, Braverman, S: Reevaluation of the Optic Oisk Vasculature. Am. J. Ophthalmol. 82(2):165-173, 1976.

29. Tansley, K: Comparison of the Lamina Cribrosa in Mammalian Species with Good and with Indifferent Vision. Brit. J. Ophthalmol. 40:178-182, 1956.

30. Frank, RN: On the Pathogenesis of Oiabetic Retinopathy. Ophthalmol. 91(6):626-634, 1984.

31. Tilton, RG, Hoffmann, PL, Kilo, C, Williamson, JR: Pericyte Oegeneration and Basement Membrane Thickening in Skeletal Muscle Capillaries of Human Diabetics. Oiabetes 30:326-334, 1981.

32. Engerman, RL, Colquhoun, PJ: Epithelial and Mesothelial Basement Membranes in Diabetic Patients and Oogs. Oiabetologia 23:521-524, 1982.

33. Leiberman, MF, Maumenee, AE, Green, WR: Histologic Studies of the Vasculature of the Anterior Optic Nerve. Am. J. Ophthalmol. 82(3):405-423, 1976.

34. Risco, JM, Grimson, BS, Johnson, PT: Angioarchitecture of the Ciliary Artery Circulation of the Posterior Pole. Arch. Ophthalmol. 99:864-868, 1981.

35. Simoens, P, Ghoshal, NG: Arterial Supply to the Optic Nerve and Retina of the Sheep. J. Anat. 133:481-497, 1981.

36. Yoshimoto, H, Murata, M, Yamagami, K, Matsuyama, S: Studies on the Angioarchitecture of the Posterior Choroid in Rat and Role of Posterior Ciliary Vein. Invest. Ophthalmol. 19(10): 1245-1250, 1980.

37. Wong, VG, Macri, FJ: Vasculature of the Cat Eye. Arch. Ophthalmol. 72:351-358, 1964.

38. Risco, JM, Nopanitaya, W: Ocular Microcirculation. Scanning Electron Microscopic Study. Invest. Ophthalmol. 19(1):5-12, 1980.

39. Prince, JH, Oiesem, CO, Eglitis, I, Ruskell, GL: Anatomy and Histology of the Eye and Orbit in Oomestic Animals. CC Thomas, Springfield, Ill., 1960.

40. Ouke-Elder, S: The Eye in Evolution, Vol. I, System of Ophthalmology, Ouke-Elder, S, ed., Henry Kimpton, London, 1958.

41. Ernest, TJ, Potts, AM: Pathophysiology of the Distal Portion of the Optic Nerve. 2. Vascular Relationships. Am. J. Ophthalmol. 66:380-387, 1968.

42. Francois, J, Neetens, A, Collettes, JM: Vascular Supply of the Optic Pathway. 2. Further Studies by Microarteriography of the Optic Nerve. Br. J. Ophthalmol. 39:220-232, 1955.

43. Levitzky, M, Henkind, P: Angioarchitecture of the Optic Nerve. 2. Lamina Cribrosa. Am. J. Ophthalmol. 68:986-996, 1969.

44. Burger, PC, Chandler, DB, Klintwork, GK: Scanning Electron Microscopy of Vascular Casts. J. Electron Microscopic Techniques 1:341-348, 1984.

45. Shimizu, I, Ujiie, K: Structure of Ocular Vessels. Igakin-Shoin. Tokyo, 1978.

46. Schraufnagel, OE, Roussos, C, Macklem, PT, Wang, N: The Geometry of the Microvascular Bed of the Diaphragm. Comparison to Intercostal and Triceps. Microvasc. Res. 26:291-306, 1983.

47. Kohler, T, Leiser, R: Blood Vessels of the Bovine Choroidea. ACTA anat. 116:55-61, 1983.

48. Ohkuma, H, Ryan, SJ: Vascular Casts of Experimental Subretinal Neovascularization in Monkeys. Invest. Ophthalmol. 24(4):481-490, 1983.

49. Burger, PC, Chandler, OB, Klintworth, GK: Corneal Neovascularization as Studied by Scanning Electron Microscopy of Vascular Casts. Lab. Invest. 48(2):169-180, 1983.

50. Anderson, BG, Anderson, WD: Microvasculature of the Canine Heart Demonstrated by Scanning Electron Microscopy. Am. J. Anatomy 158:217-227, 1980.

51. Tano, Y, Chandler, DB, Machener, R: Vascular Casts of Experimental Retinal Neovascularization. Am. J. Ophthalmol. 92:110-120, 1981.

52. Casellas, D, Mimran, A: Shunting in Renal Microvasculature of the Rat: A Scanning Microscopic Study of Corrosion Casts. Anat. Rec. 201:237-248, 1981.

53. Ducournau, DH: A New Technique for the Anatomical Study of the Choroidal Blood Vessels. Ophthalmologica 184:190-197, 1982.

54. Hogan, MJ, Feeney, L: The Ultrastructure of the Retinal Blood Vessels. I. The Large Vessels. J. Ultrastructure Res. 9:10-28, 1963.

54. Hogan, MJ, Feeney, L: The Ultrastructure of the Retinal Blood Vessels. I. The Large Vessels. J. Ultrastructure Res. 9:10-28, 1963.

55. Hogan, MJ, Feeney, L: The Ultrastructure of the Retinal Blood Vessels. II. The Small Vessels. J. Ultrastructure Res. 9:29-46, 1963.

56. Hogan, MJ, Feeney, L: The Ultrastructure of the Retinal Blood Vessels. III. The Vascular-Glial Relationships. J. Ultrastructural Res. 9:47-64, 1963.

57. Cohen, AI: Ultrastructural Aspects of the Human Optic Nerve. Invest. Ophthalmol. 6(3):294-308, 1967.

58. Minckler, DS, McLean, IW, Tso, MOM: Distribution of Axonal and Glial Elements in the Rhesus Optic Nerve Head Studied by Electron Microscopy. Am. J. Ophthalmol. 82(2):179-187, 1976.

59. Yamada, E, Shikano, S: Electron Microscopic Atlas in Ophthalmology. Igaku Shoin, Tokyo, 1972.

60. Neetens, A, Dockx, P: Fine Structure of Optic Disk and Laminar Monkey Capillaries. Microvasc. Res. 11:195-201, 1976.

61. Majno, J: Ultrastructure of the Vascular Membrane. Chapter 64, In Handbook of Physiology. Section 2: Circulation. Vol III. Editor: WF Hamilton. pp 2293-2375, American Physiological Soc. Washington, DC, 1965.

62. Wolff, JR: Ultrastructure of the Terminal Vascular Bed as related to Function, In Kaley, G, Altura, BM, (eds), Microcirculation, Vol. I. University Park Press, Baltimore, pp 95-130, 1977.

63. Levy, NS, Crapps, EE: Displacement of Optic Nerve Head in Response to Short-term Intraocular Pressure Elevation in Human Eyes. Arch. Ophthalmol. 102:782-786, 1984.

64. Ho, KL: Ultrastructure of Cerebellar Capillary Hemangioblastoma. I. Weibel-Palade Bodies and Stromal Cell Histiogenesis. J. Neuropath. and Exp. Neurol. 43(6):592-608, 1984.

65. Takeshige, Y, Fujimoto, S: Ultrastructural Modifications of Endothelial Cells by Changes of the Vascular Function. 9th Europ. Conf. Microcirculation. Antwerp 1976. Bibl. anat., No. 16, pp. 364-369, Karger, Basel, 1977.

66. Matsuda, H, Suguira, S: Ultrastructure of Tubular Body in the Endothelial Cells of the Ocular Blood Vessels. Invest. Ophthalmol. 9(12):919-925, 1970.

67. Freddo, TF, Townes-Anderson, E, Raviola, G: Rod-shaped Bodies and Crystalloid Inclusions in Ocular Vascular Endothelia of Adult and Developing _Macaca mulatta_. Anat. Embryol. 158:121-131, 1980.

68. Bertini, F, Santolaya, R: A Novel Type of Granule Observed in Toad Endothelial Cells and Their Relationship with Blood Pressure Active Factors. Experientia (Basel) 26(5):522-523, 1970.

69. Weibel, ER, Palade, GE: New Cytoplasmic Components in Arterial Endothelia. J. Cell Biology 23:101-112, 1964.

70. Krstic, R, Postic, G: Ultrastructure of Specific Endothelial Organelles (SEO) of the Iris Capillaries in Glaucoma Simplex. Microvasc. Res. 5:141-144, 1973.

71. Alm, A, Bill, A: Ocular and Optic Nerve Blood Flow at Normal and Increased Intraocular Pressure in Monkeys (Macaca irus): A Study with Radioactively Labelled Microspheres Including Flow Determination in Brain and Some Other Tissues. Exp. Eye Res. 15:15-29, 1973.

72. Geijer, C, Bill, A: Effects of Raised Intraocular Pressure on Retinal, Prelaminar, Laminar, and Retrolaminar Optic Nerve Blood Flow in Monkeys. Invest. Ophthalmol. 18(10):1030-1042, 1979.

73. Gafner, F, and Goldmann, H: Experimentalle Untersuchungen uber den Zusammenhang von Angendruchsteigerung und Gesicht-sfeldschadigung. Ophthalmologica 130:357, 1955.

74. Hayreh, SS: Glaucoma Damage. In: Heilmann, K, and Richardson, KT, editors: Glaucoma. Conceptions of a Disease. Stuttgart, George Thieme Publishers, pp. 104-137, 1978.

75. Grunwald, JE, Riva, CE, Stone, RA, Keates, EU, Petrig, BL: Retinal Autoregulation in Open-angle Glaucoma. Ophthalmol. 91:1690-1694, 1984.

76. Best, M, Gerstein, D, Wald, N, Rabinovitz, AZ, Hiller, GH: Autoregulation of Ocular Blood Flow. Arch Ophthalmol. 89:143-148, 1973.

77. Riva, CE, Grunwald, JE, Petrig, BL: Autoregulation of Human Retinal Blood Flow. Invest. Ophthalmol. 27(12):1706-1712, 1986.

78. Alm, A: Microcirculation of the Eye. In The Physiology and Pharmacology of the Microcirculation. Vol. I, Mortillaro, NA, ed., Academic Press, New York, NY, pp. 259-299, 1983.

79. Samuelson, DA: Personal communication. University of Florida, 1987.

80. Granger, HJ, Borders, JL, Meininger, GA, Goodman, AH, Barnes, GE: Microcirculatory Control Systems. In The Physiology and Pharmacology of the Microcirculation. Vol. I, Mortillaro, NA, ed., Academic Press, New York, New York, pp. 209-236, 1983.

81. Rhodin, JAG: Ultrastructure of Mammalian Venous Capillaries, Venules, and Small Collecting Veins. J. Ultrastructure Res. 25:452-500, 1968.

82. Rhodin, JAG: The Ultrastructure of Mammalian Arterioles and Precapillary Sphincters. J. Ultrastructure Res. 18:181-223, 1967.

83. Hayreh, SH: Anatomy and Physiology of the Optic Nerve Head. Trans. Am. Acad. Ophthalmol. Otol. 78:OP240-OP253, 1974.

84. Van8uskirk, EM: The Canine Eye: The Vessels of Aqueous Drainage. Invest. Opthalmol. 18(3):223-230, 1979.

85. Sharpnack, DD, Wyman, M, Anderson, 8G, Anderson, WD: Vascular Pathways of the Anterior Segment of the Canine Eye. Am. J. Vet. Res. 45(7):1287-1294, 1984.

86. Francois, J, Neetens, A: Vascularization of the Optic Pathway. 1. Lamina Cribrosa and Optic Nerve. Br. J. Ophthalmol. 38:472-487, 1954.

87. Ernest, JT, Potts, AM: Pathophysiology of the Distal Portion of the Optic Nerve. 1. Tissue Pressure Relationships. Am. J. Ophthalmol. 66(3):373-380, 1968.

88. Araki, M, Takahashi, H: Observations on the Corrosion Casts of the Retinal Capillary 8ed at the Posterior Pole and the Capillaries of the Optic Disc: Normal and Glaucomatous Eye. Acta. Soc. Ophthalmol. Jap. 81:982-994, 1977.

89. Fryczkowski, AW, Grimson, 8S, Peiffer, RL: Vascular Casting and Scanning Electron Microscopy of Human Ocular Vascular Abnormalities. Arch. Ophthalmol. 103:118-120, 1985.

90. Ernest, TJ: Retinal Circulation in Diabetes Mellitus. Arch. Ophthalmol. 104:986-988, 1986.

91. Lewis, RA, Johnson, CA, Quigley, HA: Early Detection of Glaucomatous Damage. Surv. Ophthalmol. 30(2):111-126, 1985.

92. Levene, RZ: Low Tension Glaucoma: A Critical Review and New Material. Surv. Ophthalmol. 24:621-664, 1980.

93. Gum, GG: Glycosaminoglycans in the Iridocorneal Angle of the Normal Canine and the Glaucomatous 8eagle. Ph.D. Dissertation, University of Florida, 1986.

94. Pillunat, LE, Stodtmeister, R, Wilmanns, I, Christ, TH: Autoregulation of Ocular 8lood Flow During Changes in Intraocular Pressure. Preliminary Results. Graefe's Arch. Clin. Exp. Ophthalmol. 223(4):219-223, 1985.

BIOGRAPHICAL SKETCH

I was born in Carthage, Illinois, in 1953 and graduated in 1971 from Quincy Senior High School in Quincy, Illinois. In 1974 I received a Bachelor of Science degree in biology (comprehensive) from Illinois State University in Normal, Illinois. I worked as a laboratory technician for six months for Calcium Carbonate Company in Quincy, Illinois, after graduation. I then entered graduate school in insect taxonomy at Illinois State University for one year. In 1976 I began my veterinary education at the University of Illinois in Urbana, Illinois. I graduated in 1980 and entered a small animal practice in Kingston, Massachussetts. In 1981 I accepted a National Institute of Health Training Grant in Comparative Ophthalmology at the College of Veterinary Medicine, University of Florida, Gainesville, Florida. I passed the veterinary ophthalmologist certification examination and received diplomate status in 1984. In 1985 I accepted an assistant professor position in comparative ophthalmology at the College of Veterinary Medicine, University of Tennessee, Knoxville, Tennessee, and remain there at this time. I received my Ph.D. degree (specializing in electron microscopy) from the University of Florida in 1987. I have authored or coauthored 20 scientific publications and a chapter in Current Veterinary Therapy IX. I am active in veterinary ophthalmic consulting in Tennessee and have provided continuing education in veterinary ophthalmology at

local, state and national veterinary symposia. I remain interested in comparative ocular microvasculature and will continue my research in this area.

I certify that I have read this study and that in my opinion it conforms to acceptable standards of scholarly presentation and is fully adequate, in scope and quality, as a dissertation for the degree of Doctor of Philosophy.

Darryl Buss
Professor of Animal Science and
Veterinary Medicine

I certify that I have read this study and that in my opinion it conforms to acceptable standards of scholarly presentation and is fully adequate, in scope and quality, as a dissertation for the degree of Doctor of Philosophy.

William W. Dawson
Professor of Neuroscience

This dissertation was submitted to the Graduate Faculty of the College of Medicine and to the Graduate School and was accepted as partial fulfillment of the requirements for the degree of Doctor of Philosophy.

December 1987

Dean, College of Medicine

Dean, Graduate School

UNIVERSITY OF FLORIDA
3 1262 08554 7932